SYNTHESIS AND CHARACTERIZATION OF NOVEL FLUORESCENT INJECTABLE MICRO-CARRIERS FOR TISSUE REGENERATION

A Thesis

by

AKSHI ARORA

Submitted to the Office of Graduate and Professional Studies of
Texas A&M University
in partial fulfillment of the requirements for the degree of

MASTER OF SCIENCE

Chair of Committee,	Xiaohua Liu
Committee Members,	Jian (Jerry) Feng
	Lynne Opperman
	Venu Varanasi
Head of Department,	Paul Dechow

May 2014

Major Subject: Biomedical Sciences

ABSTRACT

Specific problem: Our previous study showed that the nanofibrous poly-l-lactic acid (NF-PLLA) microspheres are excellent cell carriers for tissue regeneration. However, these injectable microspheres are not fluorescent biomaterials. Incorporation of fluorescent chromophore into NF-PLLA microspheres will allow imaging for proper delivery of scaffold at the specified site and monitor time related degradation in the scaffold, and tissue regeneration by live fluorescent imaging, without the need of sacrificing the animals or undertaking elaborate histological procedures. To date, there is no report on the synthesis of fluorescent PLLA. In this research, we aim to develop an injectable fluorescent PLLA scaffold for tissue regeneration by using Eosin Y (EY) fluorophore as initiator.

Method: The fluorescent polymer (PLLA-EY) was synthesized by ring-opening polymerization (ROP) of l-lactide by bulk polymerization method using stannous octoate $Sn(Oct)_2$ catalyst and EY fluorophore initiator, at four different monomer/initiator (M/I) molar ratios (20:1,100:1,200:1,400:1). The PLLA-EY polymer was characterized by FT-IR, UV-visible spectrophotometry and molecular weight (MW). The smooth walled (SW) and nanofibrous (NF) microspheres were fabricated from PLLA-EY 200:1 and 400:1 from methods previously described. These were characterized by SEM, confocal, *in vitro* biodegradation in PBS (pH change and SEM) and cytotoxicity testing (MTS assay) on dental pulp stem cells (DPSCs).

Results: EY initiator generated free radicals causing ROP of l-lactide and incorporation of EY in the PLLA polymer chain. FT-IR and UV-vis spectra confirmed incorporation of EY in the polymer. Increasing the M/I ratio increased MW of PLLA-EY polymer. Microspheres formed from PLLA-EY were auto-fluorescent and increasing the polymer MW resulted in more well-defined nanofibers. Both short term (7d) and long term (21d) cytotoxicity results confirmed

non-toxicity of the fluorescent polymer to DPSCs. NF microspheres formed small aggregates with cellular extensions between the DPSCs. Biodegradation of NF microspheres was not seen until 6 weeks in PBS solution under SEM.

Conclusion: Fluorescent PLLA-EY polymer and its microparticles can be manufactured, and appear to be very promising candidates for dental pulp regeneration. Future studies should evaluate the ability to track the polymer and their microparticles *in vivo*, and their ability to accommodate cell adhesion, proliferation, differentiation and *in vivo* implantation.

ACKNOWLEDGMENTS

My journey in the Biomedical Sciences Dept. at Baylor College of Dentistry has been a roller coaster ride with innumerous ups and downs, but as they say all is well that ends well. I wish to express my gratitude to many people who have been of crucial support to me.

First and foremost, my sincere thanks go to my thesis director, Dr. Xiaohua Liu. He has been a mentor, a guide and a guardian to me in these years. I am grateful to him for his unending support and encouragement, for showing faith in this project and in my working abilities in conducting research and preparing this dissertation. I also thank him for the countless hours in discussion, for being very patient and understanding with my academic, research or personal issues. Additionally, I would also thank my committee members Dr. Jerry Feng, Dr. Lynne Opperman and Dr. Venu Varanasi for their interest in my work. Their research insights in this project and critical, but insightful comments on my work greatly helped in shaping and guiding the direction of my research work. I am also grateful to them for reviewing my thesis and for their thoughtful and detailed comments.

I am deeply thankful to our Program Director, Dr. Kathy Svoboda, who has always been there for me as my second mentor. Thank you for all your help and guidance in conducting the confocal experiments, which I thought was the most challenging part of the study. Thank you for being so supportive and accommodative of me and giving me a chance to prove my abilities, when I had little hope. This thesis and my degree would not have been accomplished without her support and guidance.

I particularly wish to acknowledge my friend and ex-colleague Dr. Amanda Strom for teaching me the basics in the laboratory and for her continued assistance, advice and input along each and every step of this project. I am also grateful to my dear friend Neda Tousi Saffarian,

for all her support, guidance and help in conducting cell experiments, which I originally had no knowledge of. Special thanks to Lilly Guo for teaching me to work on the SEM and getting great images, without which my thesis would not have been complete. I am indebted to the Biomedical Sciences Department staff –Nancy Anthony, Marge Palma, Jeanne Santa Cruz, and Connie Tillberg, and all my friends and colleagues who have been like a family to me in these years, for their warmth and their unending support in some way of the other.

I am grateful to my parents, Dr. Satish K. Arora and Veena Arora for their unconditional love, support and encouragement and for making me who I am today. They have been the driving force behind all my undertakings in life and have encouraged to me to pursue each academic endeavor to the fullest. Thank you Papa, you have been my first role model!

My endeavor in life would never have been successful without the love and support of my husband Deepak and my two little munchkins- Avika and Ayush. I delivered both of them during my association with BCD. I am extremely thankful to them for their patience and understanding me even when I wasn't able to give them enough time. Thank you Deepak for your endless willingness to listen to my frustrations, for your words of advice, and most importantly, for believing in me when I didn't.

Special thanks to my in-laws, siblings, all my friends and families who have supported me throughout my academic career and have influenced me in many ways. Love you all.

TABLE OF CONTENTS

Page

Page

LIST OF FIGURES

Page

Page

1. INTRODUCTION

Fluorescence is the property of some atoms and molecules to absorb light at a particular wavelength and subsequently emit longer wavelength after a brief interval (1). The fluorescence imaging technique uses high intensity light to excite fluorescent molecules in the sample. A range of fluorescent materials are available and include organic dyes, genetically encoded fluorescent proteins, nanoparticles like carbon and silicon and quantum dots, and fluorescent polymeric materials. The high sensitivity, high resolution and safety of fluorescence imaging has led to an increasing use of fluorescent biomaterials, specifically fluorescent polymers as bio-molecular probes in molecular and cell biology as well as implant materials in tissue engineering.

Tissue engineering is "an interdisciplinary field that applies the principles of engineering and life sciences toward the development of biological substitutes that restore, maintain, or improve tissue function or a whole organ"(2). The advent of tissue engineering and regenerative medicine has revolutionized the treatment of impaired organs and missing organs and tissues due to disease, trauma, or tumors.

Biomaterials are critical components in a variety of biomedical applications including tissue engineering, drug delivery, and medical devices, the most common ones are the biodegradable polymers - polyesters, polyanhydride, polyurethane, polyphosphazenes etc. Of these polymers, the biodegradable polyesters such as polylactides, polyglycolides, and their copolymers, that are approved by the food and drug administration (FDA) for use in medical devices, are of significant interest for biological research. These polymers most commonly degrade by a hydrolysis process, in which the ester bond of the polymer breaks down in presence of water, although some polymers may also degrade by enzymatic degradation.

One of the disadvantages of using biodegradable polymers is that it is very difficult to locate these biomaterials both during and after placement in the body. Also, evaluation of time-related biomaterial degradation is not possible without elaborate invasive procedures like tissue dissection and immunohistochemistry. Imparting fluorescence to the polymer biomaterial will allow for *in vivo* imaging for placement and analysis of biodegradation as well tissue regeneration by live fluorescent imaging, without the need of sacrificing the animals or undertaking elaborate histological procedures.

This study aimed on imparting fluorescence to the biodegradable polymer poly-l-lactic acid (PLLA). The second section of this thesis is a review of the currently available fluorescent biomaterials, with an emphasis on the polymeric biomaterials. This section also reviews the injectable scaffolds including details of their types, advantages, disadvantages and use of these scaffolds in dental and craniofacial tissue engineering. The goals and aims of the research study are also included in this section. The third section includes the research related to synthesis of poly-l-lactic acid (PLLA) based fluorescent polymer and its characterization. The fourth section contains details about the synthesis of the fluorescent microspheres that were fabricated from the fluorescent polymer as well as their characterization and properties.

2. LITERATURE REVIEW ON FLUORESCENT BIOMATERIALS AND INJECTABLE SCAFFOLDS

2.1 FLUORESCENT BIOMATERIALS

Fluorescence is a luminescence phenomenon that occurs in fluorescent materials with fluorophores. In this process, a fluorophore absorbs light of a particular wavelength and then re-emits a quantum of light with an energy corresponding to the energy difference between the excited state and the ground state (3). Fluorescent biomaterials or fluorophores have gained great scientific attention in last few years due to their engrossing properties and important applications in the fields of materials and life sciences. Imaging techniques using this property of fluorescence are highly reliable and sensitive for detecting an interplay of bio-molecules with each other and with other ionic and molecular species (4).

The most widely used fluorophores for biomedical applications are both organic and inorganic types and these include:

Organic fluorophores like-

- Organic Dyes
- Intrinsic (biological) proteins
- Fluorescent polymeric materials

Some of the common inorganic fluorophores are:

- Metal ligand complexes (Lanthanides chelates)
- Carbon and silicon nanoparticles
- Quantum dots

The above mentioned fluorophores are discussed briefly in the section below.

2.1.1 Organic dyes

Synthetic organic dyes like fluoresceins, rhodamine and cyanines and the newer ones like Alexa dyes are the traditional and most established fluorescent labels (5, 6). Fluorescein was the first one to be used in biological research . Derivatives of this dye and their bio-conjugates like fluorescein isothiocyanate (FITC), rhodamine, tetramethyl rhodamine isothiocyanate (TRITC) have also been developed for improved performance. Because of their relatively small size, the dye can easily be cross-linked to larger biomolecules like antibodies without interfering with their biological function (4). Since these dyes can absorb and emit wavelengths of a wide range, they can also be used for multi-colored imaging (7). Applications of the organic dyes include as labels for biomolecules, cellular stains and as enzyme-substrates (8).

These dyes have poor photo-chemical stability and undergo rapid photo-bleaching on repeated exposure (7). Also, they possess a wide excitation and emission spectra (short stroke shift) and are associated with problems like higher background signal and greater noise to signal ratio. There *in vivo* applications are also largely limited due to associated cell toxicity (4).

2.1.2 Intrinsic (biological) proteins

These proteins are derived from biological sources as the name suggests. Green fluorescent protein (GFP), cloned from *Aequorea victoria* jellyfish, was the first biological fluorescent protein to be used for research applications (9, 10). GFP is a well-established marker for studying gene expression and protein targeting in cells and organisms (11, 12).

GFP has also been engineered to produce a vast array of mutants that are broadly referred to as genetically engineered fluorescent proteins (FPs) (13). Fluorescent proteins undergo photo-bleaching and have a low quantum yield (14, 15).

Another class of biological proteins is the phycobiliproteins which are stable and highly soluble proteins derived from cyanobacteria and eukaryotic algae (16-18). These include

fluorophores like allophycocyanin, phycocyanin, and phycoerythrins (19, 20). The broad excitation spectra of phycobiliproteins allows for simultaneous detection of more than one subpopulation of cells or intracellular organelles by a single excitation source. However, these dyes are relatively large sized, which may limit their diffusion into the cells and tissues. These are commonly used for biomedical research as fluorescent probes in immunoassays, flow cytometry and fluorescent microscopy (18).

2.1.3 Metal ligand complexes like lanthanide chelates

Lanthanide chelates are composed of an organic chromophore which is chelated to a lanthanide molecule, most commonly terbium (Tb^{3+}) or europium (Eu^{3+}) (21). The chromophore is a light sensitive 'antenna' and absorbs photons from the excitation light, which is then transferred to the lanthanide molecule (22). Lanthanide chelates have a millisecond lifetime and long decay times which results in reduced noise to signal ratio and higher detection sensitivity (21, 22). This also allows them to be useful in time resolved fluoroscopy measurements (21). The chelate can also serve as a scaffold for attaching a reactive group for coupling the biomolecules to the fluorophore (22, 23).

2.1.4 Carbon and silicon nanoparticles

Fluorescent carbon nanoparticles (FCN) composed of non-toxic carbon are promising alternatives to quantum dots for *in vivo* cell imaging applications where use of QDs is limited due to presence of toxic heavy metals (24). Highly fluorescent carbon nanoparticles with tunable visible emission have been synthesised recently for biological labeling (25).

Fluorescent silica nanoparticles (FSNPs) consist of a shell of silica NPs loaded with a core of fluorescent dye molecules (26, 27). The fluorescent molecules are somewhat protected by the surrounding silica layer, and result in good photostability and brightness (26). The surface

of FSNPs can be conjugated to specific biomolecules like drugs, antibodies etc. for drug delivery and bioimaging, respectively (28).

2.1.5 Quantum dots (QDs)

QDs are fluorescent semiconductor nanocrystals of approximate size range of 1-10 nm, which are produced from periodic groups II/VI or III/V. These nanocrystals possess a unique highly controlled and well defined spectral property because the absorption and emission wavelengths are dependent on the composition and size of the nanocrystals. Smaller particles emit shorter wavelengths and larger particles emit longer wavelengths.

In comparison to organic dyes, QDs have a continuous absorbance spectra and a sharp, well defined emission peak. Thus multicolored QDs can be excited by the same light source and signal overlap is also not a problem as with organic dyes (29, 30). These also possess higher fluorescence intensity and excellent photostability in comparison to organic dyes (29-31).

The most prominent QD materials for biological applications are CdSe and CdTe (4, 14).Their surface can be easily conjugated bio-molecular affinity ligands like antibodies, peptides as well as therapeutic drugs etc. Current biological applications include cell labeling for cellular imaging and tracking and tissue imaging for diagnostic purposes as well as agents for delivery of drugs (14, 32-34). However, the presence of heavy metals, such as cadmium and selenium for *in vivo* applications are associated with cytotoxicity and altered cell function (35, 36). Surface passivation strategies by elaborate biopolymer surface coatings have improved the biocompatibility of QDs (37-39) but their long term *in vivo* effects largely remain unknown.

2.1.6 Fluorescent polymeric materials

These are organic polymers which are gaining huge interest in field of biology and medicine. There are two ways in which a fluorescent polymer can be synthesized- the traditional method is the synthesis of a polymer backbone and conjugating the end with a fluorescent

organic dye or QDs (40, 41). Particles made with these polymeric materials offer several advantages in bio-applications over their inorganic QDs like diverse functionality (29, 30), surface modification, and a higher biocompatibility (42). In particular, photoluminscent polymers are being used for a variety of biological applications, most commonly for bioimaging and biosensing (42-45) as fluorescent probes for pathogens (42, 45) and chemo-sensors for concentration for glucose or oxygen (43, 44). Fluorescent polymers are also being used as carriers for delivery of drugs (40, 46-48) and as fluorescent molecular thermometers. Wu *et al*. synthesized a spectrum of highly fluorescent conjugated polymer dots for fluorescence imaging in live cells (49). However, the above mentioned fluorescent polymers need conjugation with a dye or quantum dots to exhibit fluorescence and each of these are associated with limitations, as mentioned previously.

A newer, more easier and economical method is to polymerize the monomer by using a fluorescent initiator, thus the conjugated system is incorporated in the backbone of the polymeric chain (41). However, since these polymers do not degrade, they are not suitable for biomedical applications like tissue engineering. We know that biodegradation is a useful parameter for scaffolds constructs used in tissue engineering because it facilitates the ingrowth of newly formed tissue. An example of such biodegradable fluorescence emitting polycaprolactone (PCL) was synthesized by Zhang *et al.* using difluoroboron dibenzoylmethane (50) as an initiator, but its behavior with cells both *in vitro* and *in vivo* are unknown.

Newer classes of fluorescent polymers are the fluorescent dendrimers containing a tetramine group, like poly (amido amine), (PAMAM), poly (ethyleneliamine)(PEI) etc, where conjugated tertiary amino group seems to be responsible for fluorescence (41).

2.2 INJECTABLE BIOMATERIALS

Tissue engineering is a highly promising approach for regeneration of tissues like bone and teeth lost due to trauma and infection. Use of injectable scaffolds, which are bioactive molecules or cells with solidifiable precursors, to inject cells and/or growth factors directly into the defect results in formation of a three-dimensional structure *in situ* (51). These scaffolds are attractive in comparison to pre-formed scaffolds because they can easily be injected and fill irregularly shaped defects and wounds with easy manipulation and minimally invasive procedures, as well as cause less patient complications and discomfort (51-53). Also they solidify by an *in situ* mechanism and can be injected in any irregular sized defect without the need for prefabrication. Since the material is injectable; it eliminates the need for surgical interventions (51). The injectable scaffolds serve as ideal carriers for delivery of cells and bioactive molecules since it is much easier to incorporate these in a solution or suspension.

2.2.1 Materials used as injectable scaffolds

A variety of materials have been proposed for use as injectable scaffolds. These can be derived from natural sources or can be synthetically made in the laboratory. The natural polymers, derived from natural resources mimic properties of natural ECM and have the advantage of being easily recognized by the biological environment (54, 55). They are highly biocompatible, biodegradable and do not cause inflammatory or immune responses (55). Examples are collagen, gelatin, chitosan, hyaluronic acid, alginate, fibrin etc. However, there are concerns with these materials regarding pathogen transmission and availability in insufficient amounts for clinical applications. This has led to vast research in the field of synthetic polymers as substitutes to natural derived polymers for tissue engineering.

The properties of synthetic biomaterials can be easily tailored to demands of clinical applications. Also, they can be manufactured on a large scale. These include Poly-ethylene

glycol (PEG), Poly(α-hydroxyesters) like (PLA, PGA, PLGA), Poly(N-isopropyl acrylamide), pluronic block copolymers etc.

The third category of materials is based on ceramics and is also widely being used especially for bone tissue engineering. Ceramic materials are compounds of Ca^{2+} and PO_4^{3-} ions in varying proportions and include hydroxyapatite (HA) Hydroxyapatite (HA) (56, 57), tri-calcium phosphate (β-TCP) and calcium phosphate cements (CPC) (58-60). These inorganic materials could be used alone or can be blended with polymeric matrices, and are called hybrid materials. The blends are beneficial because they combine optimal properties of both the groups.

A new class peptide based materials called self-assembling peptides (SEPs) are gaining interest for tissue engineering and protein delivery in the past few years. These are physically cross linked structures which undergo gelation by non-covalent self-assembly mechanism (61, 62) . Since the self-assembled structures have specific functions, this property can be exploited to synthesize synthetic molecules for different tissue regeneration and drug delivery applications (63).

2.2.2 Requirements of injectable scaffolds

Injectable hydrogels should be maintained as a liquid before *injection*, but form a gel structure upon contact with body fluids. Additionally, the liquid solution can also be incorporated with growth factors (e.g., TGF and BMP) and cells (e.g., mesenchymal stem cells) (64). The injectable hydrogels and any additives like initiators, cross-linkers should be *non-toxic* before, during and after injection (65). The gel should have mild solidification conditions, such as neutral pH and physiological temperature (66). Moreover, the material, its components and any degradation products must be *biocompatible i.e.*, they should not elicit an unresolved inflammatory response nor demonstrate extreme immunogenicity. Scaffolds should also possess sufficient *mechanical strength* to withstand biomechanical loading and provide necessary

support for the cells, and should match those of the tissue at the site of implantation (67, 68). The mechanical integrity of the scaffolds mainly depend on the original rigidity of polymer chains, types of crosslinking molecules and the cross-linking density, and swelling as result of hydrophilic/hydrophobic balance (66, 69-72). The mechanical properties may be improved by incorporating particles of ceramic materials, such as β-tricalcium phosphate, hydroxyapatite, (66, 73), and by incorporating nanofibers etc. into the hydrogels (74).

Of the most critical and challenging issues in tissue engineering is the *biodegradation* of scaffold biomaterials. Ideally, degradation of scaffolds should match the rate of new tissue formation (75). The hydrogels can be degraded by three mechanisms - simple dissolution, hydrolysis, or enzymatic cleavage (66, 67, 76, 77), of which hydrolytic degradation is the most common mechanism (77). The key factors that determine the degradation rate are polymer type, the nature of crosslinking, cross-linking density, molecular weight, morphology, porosity, and amount of residual monomer (67, 68, 78, 79). Other factors, such as the local pH and incorporation of filler, may also play a role (80, 81).

2.2.3 Types of injectable scaffolds

Most common type of injectable scaffolds are the **hydrogels** which are soft and elastic polymers that form highly cross-linked three-dimensional water insoluble networks (40, 72, 82, 83). These are relatively low-viscosity aqueous solutions (sol state) prior to injection, but rapidly convert into gel (gelation) by crosslinking of adjacent polymer chains. These can be classified based on the method of crosslinking into physical hydrogel and chemical hydrogel.

Physically cross-linked hydrogels are formed by self-assembly of polymer chains which occur by a change in environmental conditions, such as temperature (chitosan, gelatin, and synthetic PNIPAAm , pluronic); ionic concentration; or pH etc. (84-86). The polymer chains are linked by physical forces like hydrogen bond (PEG/PAA inter-penetrating polymer networks

(IPN)) (87), ionic bond (alginates) (88), or hydrophobic or van der Waals interactions. In contrast, in chemically cross-linked hydrogels, covalent bonds are formed between different polymer chains through some type of reaction between adjacent functional moieties including disulfide bond formation, or reaction between thiols and acrylate or sulfones (85). External cross-linking agents most commonly glutaraldehyde can also be used for crosslinking amine-based polymer chains as well as hydroxyl group or carboxyl group of polyvinyl alcohol (89), gelatin (90), partially acetylated chitosan (91), or hyaluronic acid (92).

Another form of injectable scaffold is **microspheres** which are small particles of size (approximately between 1 and 1000μm) so that they can be injected through a syringe. These microspheres are synthesized from polymers like biodegradable aliphatic polyesters, which offer advantages of good mechanical properties, low immunogenicity and toxicity, and an adjustable degradation rate (93). The microspheres are widely being used as injectable vehicles for delivery of drugs, proteins, growth factors (93, 94) and injectable scaffolds in tissue engineering for three dimensional biomimetic cellular growth and guidance (95, 96).

There are several techniques utilized for the preparation of microspheres, such solvent evaporation (single or double emulsion solvent evaporation), spray drying technique, hot melt, solvent removal, and phase inversion microencapsulation (97-100). Solvent evaporation method is the most common method.

The microspheres can be either dense or hollow (101), and can be single-walled or multi-walled microspheres (102). Double or multi-walled microspheres have been developed to provide specific drug release properties, e.g., pulsed release, which could not be obtained by single walled-microspheres. Liu *et al*. synthesized nanofibrous hollow microspheres from star-shaped biodegradable PLLA and used it as an injectable cell carrier for cartilage regeneration in critical-size rabbit osteo-chondral defects (52). It is also possible to alter the size of the

microspheres by various techniques. Factors that could affect the particle size include the polymer content, molecular weight, sonication time, concentration of surfactant content (103). It has been found that microsphere size has a significant effect on drug release rate, and that the release rate decreases with an increase in microsphere size. Therefore, sphere sizes can potentially be varied to design a controlled drug delivery system with desired release profiles (104).

2.2.4 Development of advanced injectable scaffolding system

Incorporate bioactive molecules in injectable scaffolds

Some hydrogels that are made of non-cell interactive materials can be modified by incorporating cell membrane receptor ligands into the hydrogel matrix to improve their biofunctionality and therefore, guide cell differentiation, proliferation and migration. Alginate was covalently modified with an RGD peptide containing the amino acid sequence arginine-glycine-aspartic acid (Arg-Gly-Asp) (105), and that peptide-modified alginate showed improved osteoblast adhesion and spreading (106, 107). The Anseth group has developed a RGD with a spacer arm sequence covalently tethered to the PEG network as a pendent functionality, which gave higher survival rate of human mesenchymal stem cells than that survival seen with dually attached RGD (107, 108). PEG hydrogels have been modified by the Hubbell group and many others, with a variety of bioactive molecules to mimic the natural ECM, and to modulate specific cellular responses, such as cell adhesion, enzymatic degradation, and signal molecule-binding (109-112).

Cell-instructive scaffolds

Lutolf *et al.* engineered PEG hydrogels containing a combination of cell adhesion ligands (RGDSP) and substrates for matrix metalloproteinase (MMP) as linkers between PEG chains for delivery of recombinant human bone morphogenetic protein-2 (rhBMP-2) to

regenerate bone (113). Other bioactive molecules that enable interactions with cationic amino acids of proteins, such as growth factors, cytokines and cell adhesion molecules such as polysaccharides- HE800 (hyaluronic acid-like polysaccharide) and GY785 (GAG-like polymer) have also been explored to be beneficial for bone and cartilage tissue engineering (114).

Nanofibrous microspheres

Development of 3D nanofibrous PLLA (NF-PLLA) scaffolds is another step toward mimicking the ECM (115). Liu *et al.* has developed nanofibrous hollow microspheres self-assembled from star-shaped poly (L-lactic acid) (SS-PLLA), exhibiting the extracellular-matrix-mimicking architecture. These nanofibrous hollow microspheres were successfully used as an injectable cell carrier for chondrocytes and showed a significant improvement in cartilage repair compared to the group that used chondrocytes only (116). Also, a thermally induced phase separation method with porogen leaching was used to prepare three dimensional nanofibrous gelatin scaffolds (3D-NF-GS) and to mimic the physical architecture and chemical composition of natural bone ECM. Incubation of 3D-NF-GS with bone-like apatite showed enhanced pre-osteoblast cell differentiation (117).

2.2.5 Applications of injectable scaffolds in dental and craniofacial tissue regeneration

Injectable scaffolds are widely being used for regeneration procedures in dental and craniofacial tissues. These are excellent carriers for **pulp and dentin regeneration** owing to small size and limited access to these defects. Also, they are promising candidates for scaffolding materials in research studies related to *de novo* pulp and dentin regeneration. In these methods, the pulp stem cells are seeded into an *in vitro* scaffold and inserted into the empty canal space to allow for *de novo* growth and differentiation of cells (118-120). The stem cell lines that have been used for dentin/pulp regeneration include the postnatal dental pulp stem cells (DPSCs) (121, 122), stem cells from exfoliated deciduous teeth (SHED) (123), periodontal ligament stem

cells (124, 125), stem cells from apical papilla (SCAP) (126-128) and dental follicle progenitor cells (129, 130). DPSCs, SHED and SCAP are potentially more suitable cell sources for pulp/dentin regeneration because they are derived from pulp tissue or the precursor of pulp (118).

Periodontal or alveolar bone regeneration has shown improvement in *in vivo* studies with injectable materials incorporated with growth factors like PDGF, IGF, TGF, and recombinant human growth / differentiation factor-5 (rhGDF-5) to the scaffolds (MSC) (131-134). Ji *et al*. used this novel hydrogel of chitosan and quaternized chitosan by mixed with α-β glycerophosphate (α-β GP)(CS-HTCC/GP) as an injectable local carrier of drug the ornidazole(135) and human periodontal ligament cells (HPDLCs) and growth factor (136) for periodontal treatment *in vitro* and *in vivo*, respectively. Addition of HTCC slowed the drug release and improved its biocompatibility. *In vivo* injection of hydrogel with HPDLCs significantly enhanced their proliferation. Conjugation with bFGF further improved the regeneration potential.

Restoration of **craniofacial bone and cartilage defects** is very challenging and represents a substantial clinical problem of both medical and engineering concern. Various hydrogel polymer systems have been evaluated and appear promising as injectable scaffolds for delivery of cells, growth factors and bioactive molecules for craniofacial bone defects. Burdick *et al.* (137) attached adhesive Arg-Gly-Asp (RGD) peptide sequences to non-adhesive PEG hydrogels and photoencapsulated rat calvarial osteoblasts in these gels. The cells showed improved cell adhesion, spreading and mineralization compared with controls. Zhao *et al.* developed a composite injectable scaffold construct of CPC paste and alginate microbeads and encapsulated the human umbilical cord mesenchymal stem cells (hUCMSCs) for regeneration of

bony defects (138). This system was mechanically sound for load bearing and also enhanced osteogenic expression markers.

Other common anomalies of craniofacial regions are the **craniosynostotic defects** occurring in newborns. The Tgfs play an essential role in bone biological processes including suture patency and fusion. Due to short half -life of TGF-β3, slow and continuous release systems levels of TGF-β3 levels are ideal for suture patency. Studies by Opperman and group have shown that the patency of sutures can be maintained for upto 12 weeks by delivery of TGF-β3 through slow resorbing collagen gel at the suture site (139, 140). In a similar context, Moioli *et al.* developed a sustained release injectable system of TGF-β3 encapsulating PLGA microparticles. The release kinetics showed that TGF-β3 release was maintained even after 7 weeks. Bioactivity of TGF-β-PLGA microspheres cultured *in vitro* with the hMSCs was verified by reduced ALP activity and inhibition of osteogenic differentiation of the cells (141).

2.3 GOAL OF THE RESEARCH

Our previous study has shown that the NF PLLA microspheres are excellent cell carriers for tissue regeneration. However, these injectable microspheres are not fluorescent biomaterials. Therefore, they cannot be accurately tracked during injection and the later degradation without using invasive procedures such as tissue dissection and immunohistochemistry. By incorporating fluorescent chromophores into NF PLLA microspheres, it will allow imaging for proper delivery of scaffold at the specified site and to monitor the time related degradation changes in the scaffold as well tissue regeneration by live fluorescent imaging, without the need of sacrificing the animals or undertaking elaborate histological procedures (142-144). To date, there is no report on the synthesis of fluorescent PLLA.

In this research, we aim to develop an injectable fluorescent PLLA scaffold for tissue regeneration. We will synthesize novel fluorescent PLLA by using a fluorescent initiator,

fabricate it into fluorescent nanofibrous microspheres, and evaluate this novel fluorescent biomaterial as an injectable scaffold *in vitro* with the dental pulp stem cells (DPSCs).

2.4 AIMS OF THE RESEARCH

The following are the aims of the current study-

- **Aim 1:** Synthesis of fluorescent PLLA polymer initiated with a fluorescent initiator and its characterization
- **Aim 2:** Fabrication of microspheres (smooth walled and nanofibrous) from the fluorescent PLLA polymer initiated with fluorescent initiator and its characterization

2.5 HYPOTHESIS

The following are the hypothesis set for the study-

- **Hypothesis 1:** Polymerization reaction of lactide with fluorescent initiator will result in formation of an auto-fluorescent biodegradable polymer.
- **Hypothesis 2:** The auto-fluorescent polymer will be successfully used for fabricating nanofibrous microspheres with high quality fluorescence.

3. SYNTHESIS OF THE FLUORESCENT POLYMER AND ITS CHARACTERIZATION

3.1 MATERIALS AND METHODS

For synthesis of the fluorescent polymer, the l-lactide monomer was first recrystallized to remove any impurities. It was polymerized in bulk by ring opening polymerization (ROP) in the presence of a fluorescent initiator and a catalyst. The obtained crude polymer was dissolved in a suitable solvent, washed multiple times and finally air dried.

The l-lactide monomer (3,6-Dimethyl-1,4-dioxane-2,5-dione) (≥98%) with a melting point of 49°C (120°F) was purchased from Sigma-Aldrich (Figure 1A). The catalyst was tin (II) 2-ethylhexanoate 95% [aka Stannous octoate $Sn(Oct)_2$] (Sigma-Aldrich) (Figure 1B) which is most commonly used catalyst for ROP.

The fluorescent initiator was Eosin Y (EY) (2′,4′,5′,7′-Tetrabromofluorescein) (Sigma-Aldrich). Eosin Y is a xanthene type fluorescent dye which has gained interest as a fluorescent material owing to its moderate electronic excited state (Es 53.16 kcal/mol) (145). It is a reddish brown powder with a molecular weight of 647.89 g/mol and a melting point of 300^{o}C (572^{o}F) (146). The chemical formula is shown in Figure 1C. The optical absorption spectra of Eosin Y in basic ethanol solution shows a peak at 525nm and emits at about 544nm (147). It is soluble in ethanol (solubility 1mg/ml), methanol and acetone (147). It is insoluble in water but its potassium and sodium salts are water soluble.

3.1.1 Recrystallization of lactide monomer

Recrystallization of monomer is an important step to obtain high molecular weight polymer. For this process, first the l-lactide monomer (20 g) was dissolved in 15 ml of toluene (approx. 4:3 wt/wt%) by stirring on a hotplate at about 70°C. The dissolved monomer was

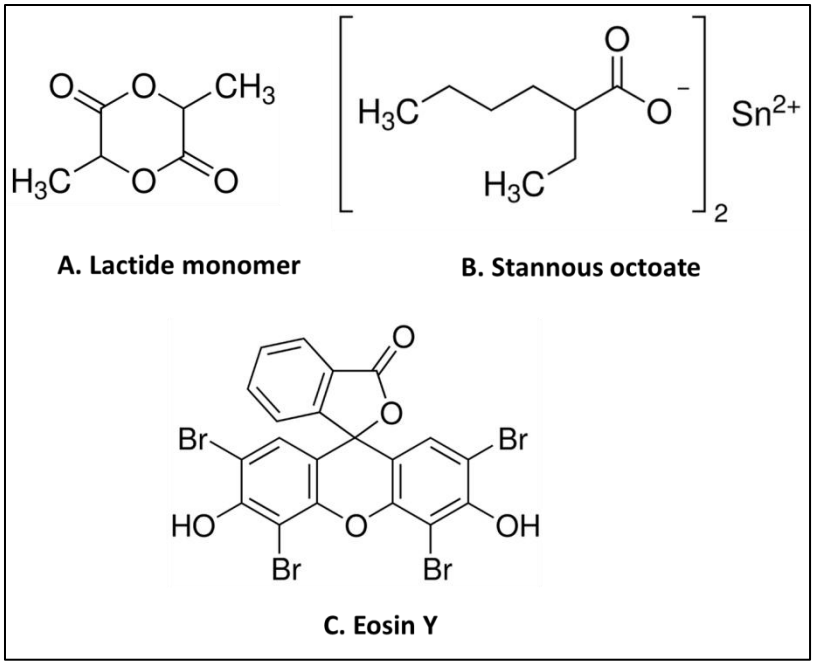

Figure 1. Chemical structures of the materials used in ROP of l-lactide (148)

removed from the heat and quickly filtered through a Buckner funnel. It was allowed to cool at ambient temperature and then kept in to the refrigerator overnight (4^{o}C) for crystal formation. This process was repeated one more time. The obtained crystals were dried for 24 hrs under reduced pressure and stored in vacuum in desiccator over copper sulphate ($CuSO_4$) desiccant to avoid the absorption of water.

3.1.2 Ring opening polymerization of l-lactide monomer

As discussed in the literature review section, one way to polymerize the lactide is by ring opening polymerization. The monomer to catalyst molar ratio i.e. l-lactide to $Sn(Oct)_2$was kept constant at 100:1 throughout the course of the polymer synthesis. However, the molar ratio of monomer to initiator (M/I) *i.e*. l-lactide to EY was altered. The following M/I ratios were synthesized depending on the requirement of the reaction- 20:1, 100:1, 200:1 and 400:1.

A double-neck round-bottomed flask was thoroughly washed and dried in the oven. L-lactide and Eosin Y were weighed in the desired amounts and placed in the flask with a clean magnetic stirrer. The flask was sealed with a septa and copper wire and vacuum-evacuated overnight. The removal of water from the system is a critical step for obtaining high-molecular-weight polymer since water, if present may act as a co-initiator. $Sn(Oct)_2$ was dissolved in dichloromethane (DCM) solution and introduced into the flask using a syringe with a stainless steel needle under N_2 purging. The DCM was later distilled under reduced pressure for about 30 min. All the work was performed in a fume hood.

The flask was conditioned in a silicone oil bath at 140°C for few minutes. The entire flask was then submerged in the silicone bath. Both the silicon bath and the monomer were stirred at 140°C overnight. After the polymerization was completed, the hot plate was turned off and the contents were allowed to cool down to room temperature (25°C). The obtained polymer was dissolved in dichloromethane (DCM) while stirring continuously. It was reprecipitated in cold methanol and then dissolved in DCM. This process was repeated about 3 times. The resultant powder / fibrous polymer were washed multiple times in absolute ethanol to remove unreacted EY and low molecular weight polymer. It was allowed to air dry for a couple of days before use. The polymer was stored in dark under reduced pressure and in vacuum in a desiccator over $CuSO_4$beads to avoid the absorption of water.

3.2 METHOD FOR CHARACTERIZATION OF THE PLLA-EY POLYMER

3.2.1 Fourier transform infrared spectroscopy (FT-IR)

FT-IR spectra for PLLA, EY and the PLLA-EY polymer samples were recorded in the ATR mode with the help of Nicolet™ iS™10 FT-IR Spectrometer (Thermo Scientific) in the range of 4000 to 600 cm^{-1}. This method determines the molecular structure of compounds based on their characteristic absorption of infrared radiation. DCM was used as a solvent for PLLA and

PLLA-EY in a concentration of 10mg/ml, whereas pure EY was dissolved in methanol. The sample drop was placed on the NaBr crystal pellet and the solvent was allowed to air dry. After proper background removal and baseline corrections the corrected the peaks were determined using Ominic software installed in the FTIR spectrometer.

3.2.2 UV-visible spectroscopy

With this method, the light absorption of a colored solution is measured at wavelengths in the near ultraviolet and visible portions of the spectrum. UV-visible spectrum measurement was done with a Cary Win 50 UV-Vis spectrometer. Firstly serial dilutions of EY were prepared (in ethanol) and a spectrum was taken to determine the absorbance peak of EY. Then, PLLA-EY polymer was dissolved in DCM and subjected to UV-visible spectral measurements**.** Corrected peaks were determined after proper background removal and baseline corrections.

For 20:1 PLLA-EY polymer, UV-visible spectroscopy was done at 5 different concentrations (2mg/ml, 5mg/ml,. 10mg/ml,. 15mg/ml, 20mg/ml).The three polymers with different M/I ratios (20:1, 100:1, 200:1) were tested at the same concentration (10mg/ml).

3.2.3 Gel permeation chromatography (GPC) for molecular weight determination

Gel permeation chromatography (GPC) is a size exclusion chromatography, used to determine the molecular weight of the polymer samples. HPLC grade tetrahydrofuran (THF) was used as an eluent (mobile phase) at room temperature at the flow rate of 1 mL min^{-1} against polystyrene (PS) standards (stationary phase). 1gm polymer samples were dissolved in 1 ml of THF for complete dissolution. The columns were equilibrated and run at 30ºC, at a flow rate of 1 ml/minute. A two-channel UV detector and a refractive index detector were used to analyze the sample data based on polystyrene standards.

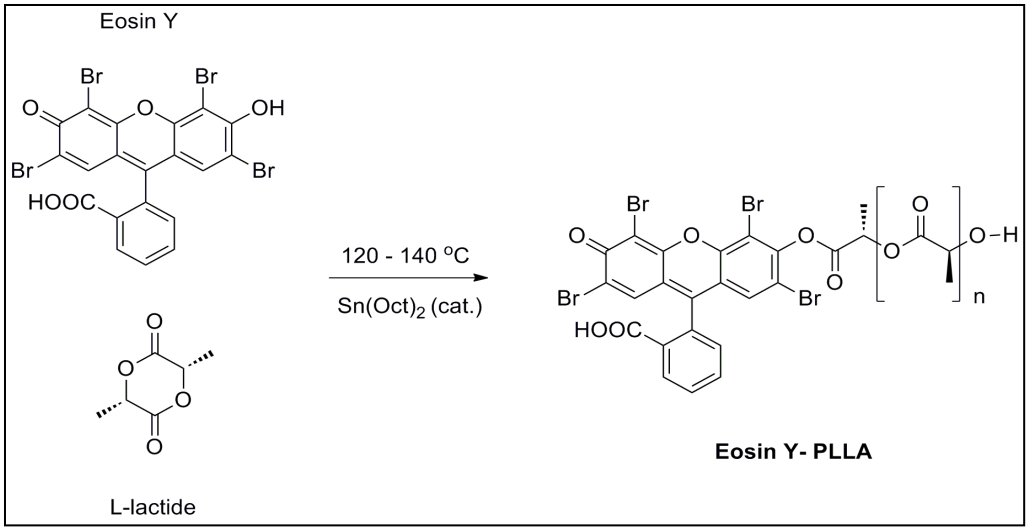

Figure 2. Chemical reaction showing the ring opening polymerization (ROP) of l-lactide with Eosin Y initiator and the formation of PLLA-EY polymer

3.3 RESULTS

3.3.1 Predicted mechanism of ROP of lactide

The chemical formulas and predicted chemical reaction and final PLLA-EY polymer is shown in the Figure 2. In the presence of $Sn(Oct)_2$ catalyst and Eosin Y initiator, the ring structure of l-lactide opens up and EY gets incorporated in the l-lactide molecule. This is followed by chain propagation with addition of more l-lactide molecules to the polymer chain.

3.3.2 Fourier transform infrared spectroscopy (FT-IR)

FT-IR spectra of PLLA, EY and PLLA-EY 20:1 is presented in the figures below. The FT-IR curve of PLLA (Figure 3) looks similar to that described in previous studies. The spectra exhibited characteristic absorption peaks at 2996 cm^{-1} for −CH stretching, 1755 cm^{-1} for −C=O stretching, 1454 cm^{-1} for $-CH_3$ bending, and 1181 cm^{-1} for −C−O−C− vibration.

FT-IR spectrum of EY is shown in Figure 4. The peaks from 3500-3200 cm^{-1} are the absorption bands for –OH stretching. The band at 1749 cm^{-1} is assigned for −C=O stretching of a

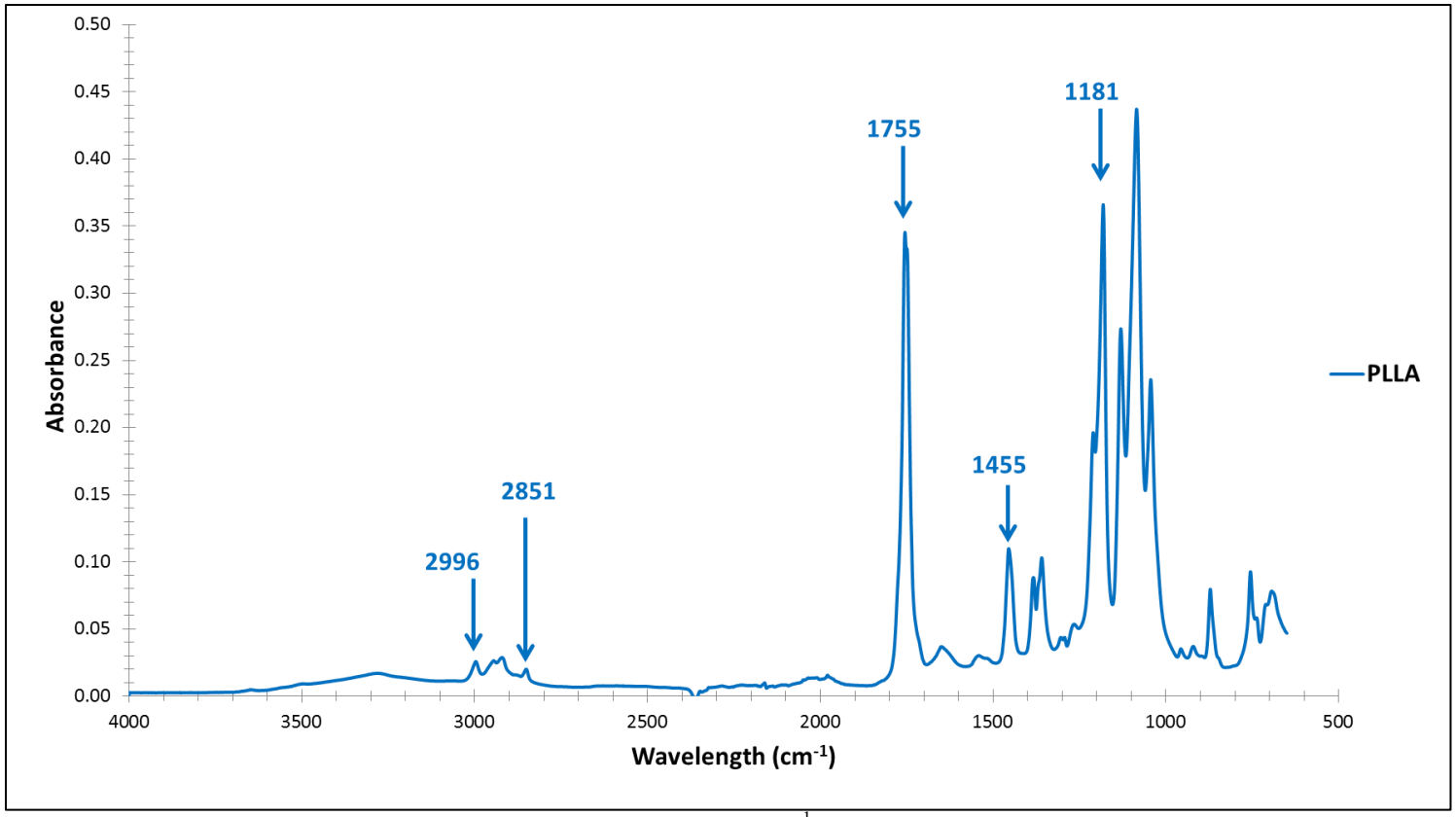

Figure 3. FT-IR spectrum of PLLA showing absorption peaks (cm^{-1})

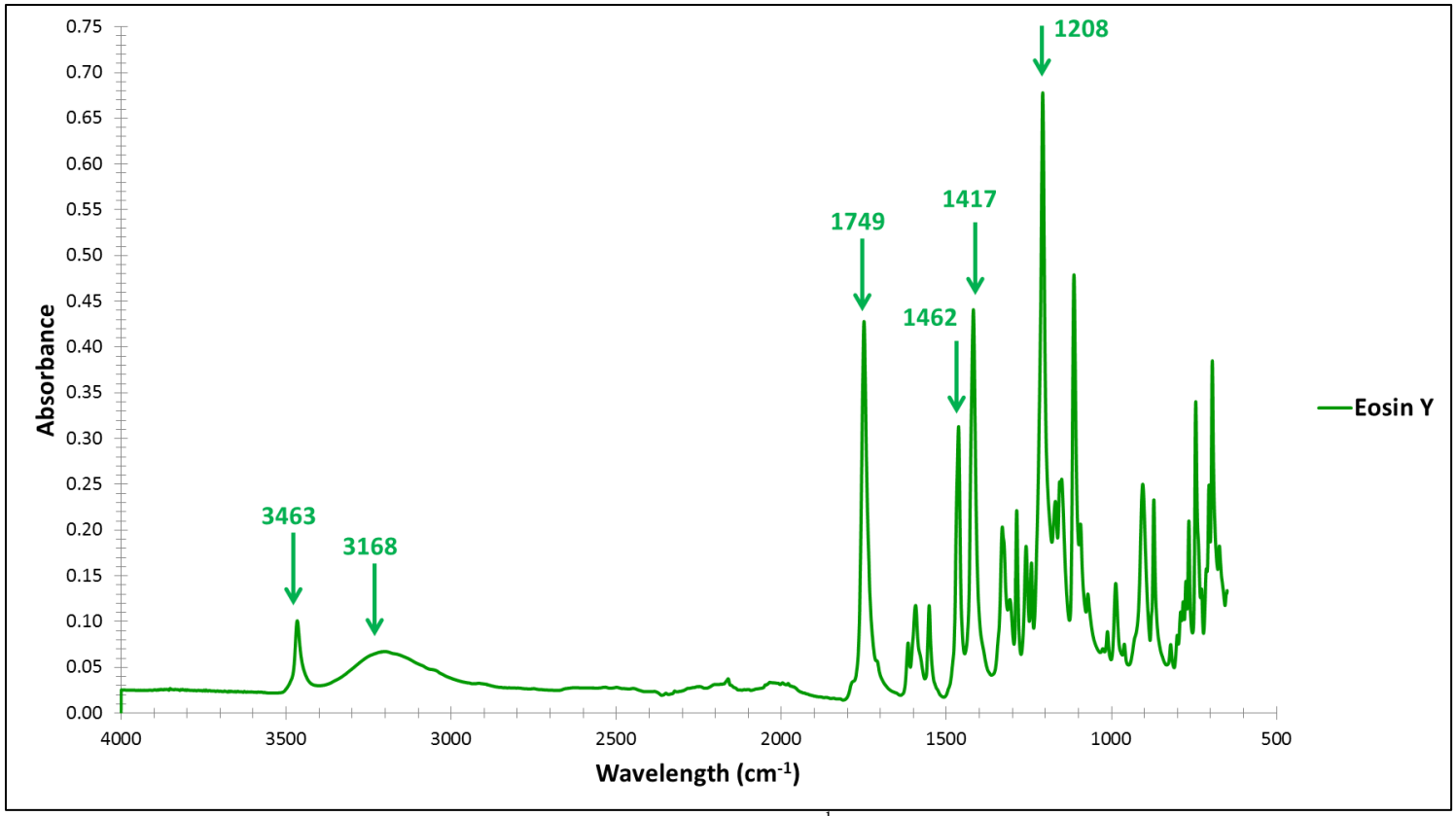

Figure 4. FT-IR spectrum of Eosin Y showing absorption peaks (cm^{-1})

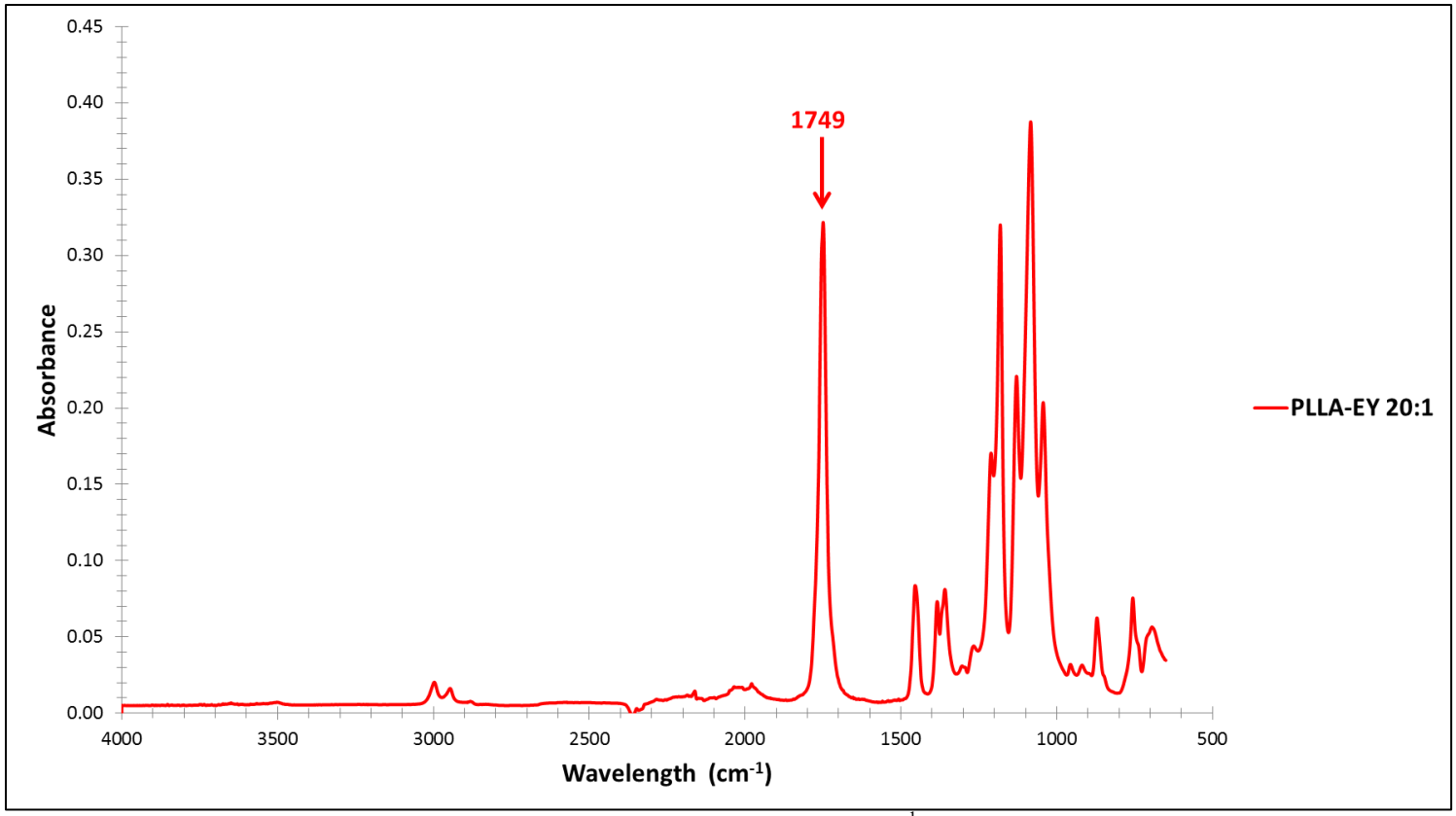

Figure 5. FT-IR spectrum of PLLA-EY 20:1 showing absorption peaks (cm^{-1})

free carboxyl group. The peaks at 1462 and 1417 cm^{-1} are from C-C stretching in a ring and from CH_3 bending.

The curve for PLLA-EY 20:1 follows PLLA curve for most of the time, as seen in Figure 5, indicating that it's a polymer of PLLA. However, the peak at 1748 cm^{-1} is very similar to that present in EY due to carbonyl stretching and indicates the presence of EY in the polymer.

3.3.3 UV-visible spectroscopy

Serial dilutions of EY solution (in ethanol) showed a peak at 524 nm indicating the absorbance wavelength of EY (R^2=0.9974).

Figure 6A represents the UV–visible spectrum of PLLA-EY polymer with different M/I ratio at same concentration (10mg/ml). The maximum absorbance was seen for 20:1 PLLA-EY (0.71; 538nm) and decreased gradually with increasing M/I ratio, indicating a decrease in the amount of initiator. A slight red shift was also observed with increase in M/I ratio.

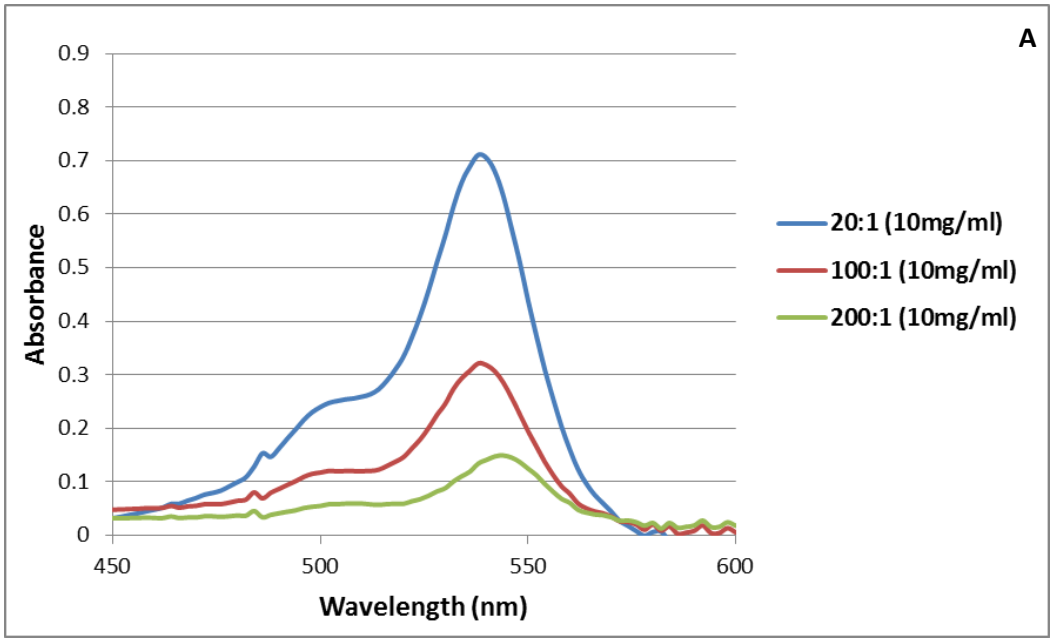

Figure 6. A) UV-visible spectrum of PLLA-EY with different M/I ratios at same concentration; B) UV-visible spectrum of PLLA-EY 20:1 at different concentrations

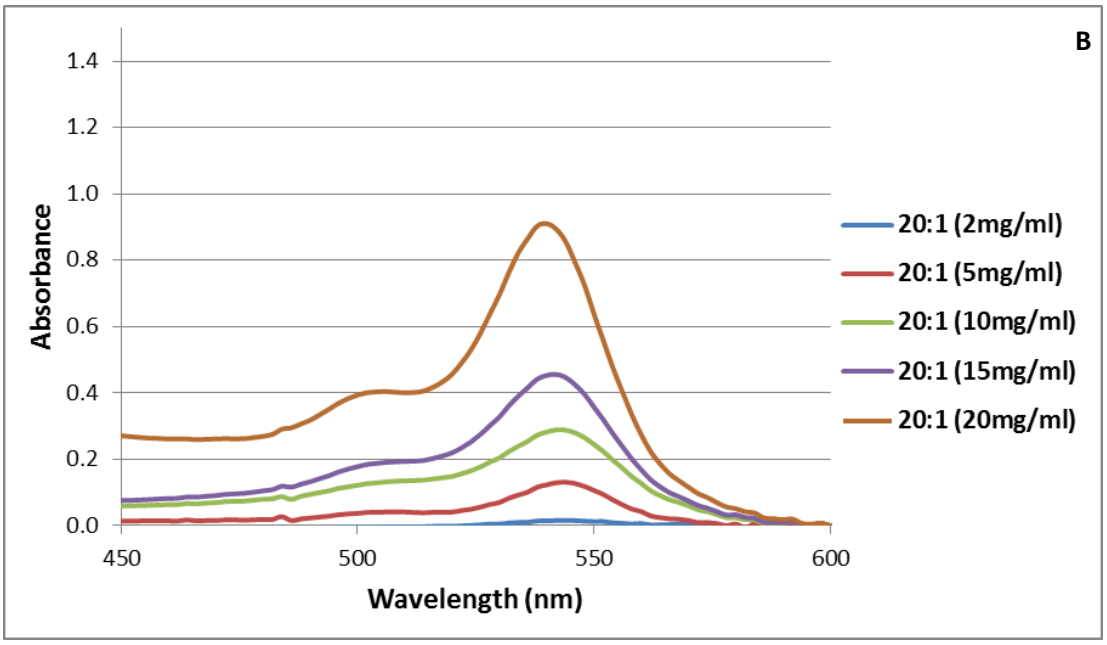

Figure 6. Continued

Figure 6B represents the UV–visible spectrum of 20:1 PLLA-EY polymer at different concentrations. The maximum absorbance was seen with 20mg/ml (0.9; 538 nm) and decreased with decreasing concentration of polymer, indicating a decrease in the initiator. A red shift was also observed with increase in M/I ratio compared to pristine EY.

The above data indicates that firstly, the EY is present in the polymer and secondly, increasing the M/I ratio decreases the amounts on initiator in the polymer.

3.3.4 Gel permeation chromatography (GPC) for molecular weight determination

Retention times of different polymers with GPC are given in Table 1. The retention times (RT) of PLLA was 8.48, PLLA-EY 400:1 was 10.32 and for PLLA-EY 100:1 was 11.23. With PLLA-EY 200:1, a peak was seen at RT 10.9. Based on the RT, the molecular weights for PLLA was about 100K, PLLA-EY 400:1 was about 3000, PLLA-EY 200:1 was about 2100 and or PLLA-EY 100:1 was about 500. Very low molecular weights were obtained for the polymers

	Retention time (RT)	Molecular Weights
PLLA-EY (400:1)	10.327	**2938**
PLLA-EY (200:1)	10.5	**2107**
PLLA-EY (100:1)	11.23	**518**

Table 1. Retention times and molecular weights of the synthesized PLLA-EY polymers determined by GPC

the molecular weight of 20:1 PLLA-EY was not calculated since the retention time would be higher than that of the standard curve that was prepared.

3.4 DISCUSSION

The PLLA be synthesized by two different routes – by polycondensation of α-hydroxycarboxylic acids, for example lactic acid for PLLA (149) or by ring-opening polymerization (ROP) of cyclic diesters. In the polycondensation reactions, water is released as a byproduct which limits the molecular weight of the polymer, therefore ROP is usually the preferred method for synthesizing high-molecular-weight polymers as those desired for biomedical applications (149, 150). ROP method also allows for a greater control of the polymerization and for controlling the monomer sequence and side chains (150). ROP can be done by using different initiators and it is also possible to obtain PLLA with different terminal groups. The bulk polymerization of lactide is done using a catalyst, and most common one is $Sn(Oct)_2$. Tin compounds are preferred for the bulk polymerization of lactide due to higher solubility in common organic solvents and in melt monomers. They also possess a high catalytic activity (reaction occurs in few hours) and lower rate of racemization of the polymer. The conversion rates are also high and high molecular weights polymers are formed (151). Initiators,

such as 1-dodecanol, glycerol and 1,4-butanediol (149) have been used for polymerization of polylactide. However, the synthesis of self-fluorescent polylactide by using florescent initiator has not been reported in the literature till date.

In this study, the aim was to synthesize PLLA by ROP of lactide in the presence of $Sn(Oct)_2$ catalyst and a fluorescent initiator-Eosin Y, based on a previous study (152). The polymerization of lactic acid in presence of $Sn(Oct)_2$ catalyst occurs by a coordination-insertion mechanism (150, 153, 154) . Eosin Y contains one free hydroxyl group and one carboxyl group. The free hydroxyl group has the capability of initiating the ROP. Based on the previous studies on lactide polymerization, we believe that the –OH group on 3'position of EY acts as a site of initiation and generates a free radical. Two molecules of EY coordinate with $Sn(Oct)_2$ and form covalent tin(II) alkoxides. This is followed by the coordination of lactide to the metal center. The insertion occurs in two steps- first, the nucleophilic attack of this alkoxide on the coordinated lactide and this result in ring opening of lactide. This causes the insertion of lactide to –OH group of EY, generating a linear monomer. The linear polymer then starts the chain propagation step.

Molecular weight of the polymer is an important property which dramatically affects its physical characteristics. As mentioned in the polymer synthesis, the recrystallization of lactic acid is an important step to obtain high molecular weight PLLA. Presence of impurities like water, methanol, ethanol etc. in the monomer can act as co-initiators for polymerization and result in low molecular weight; therefore, it is very important to minimize the water content in the reaction system to control the molecular weight of the resulting polymer.

Another way to control the molecular weight of the polymer is by altering the molar ratio of monomer to initiator (155). In this study, the PLLA was synthesized by using a range of monomer to initiator molar ratios (M/I). As the M/I ratio increases, the molecular weight of the

polymer increases, as seen in previous studies. The reason in that lower initiator amount results in less initiation sites for lactide attachment, so during chain propagation step, more lactide continue to attach to the same chain, resulting in high molecular weight polymer. In the current study, PLLA EY 100:1 had the lowest molecular weight, whereas 400:1 had the highest molecular weight. It was also seen that the physical form of 20:1 polymer was in form of a powder, and as the M/I ratio increased, the polymer became more fibrous looking, as seen in previous studies. This observation also supported the increase in molecular weights of the polymer, as obtained from GPC.

The molecular weights of the polymers synthesized in the current study were on the lower side than expected. Although the low molecular should not be an issue considering the clinical use of this polymer in pulp tissue regeneration, high molecular weights are desirable for polymer scaffolds used for bone and cartilage regeneration. Further studies should concentrate on obtaining high molecular weight PLLA-EY polymers by controlling the purity of both the lactide monomer and initiator and by standardizing the polymerization reaction conditions like temperature, pressure, polymerization time etc.

The FTIR of 20:1 showed a slight peak due to presence of Eosin Y in it at 1749$cm^{-1.}$ The FT-IR was also run for other polymers (100:1, 200:1, 400:1) but the curve was similar to PLLA and detection of EY could not be done by IR spectroscopy. This does not mean that Eosin Y was not incorporated in these polymers, but it can be concluded that the electron vibration method for detection was not sensitive enough to detect the EY through FTIR. For the same reason, UV spectrometry was done for detection of EY in the polymer and the absorption peaks of EY seen in the UV spectra confirmed the incorporation of EY in the PLLA polymer.

4. FABRICATION OF MICROSPHERES FROM FLUORESCENT PLLA-EY POLYMER AND THEIR CHARACTERIZATION

4.1 MATERIALS AND METHODS

The PLLA-EY polymers (PLLA-EY 200:1 and 400:1) were used for synthesis of two types of microspheres- smooth-walled (SW) and nanofibrous (NF). The aim of this experiment was to synthesize and characterize the microspheres and compare the differences between the two types of polymers and two types of microspheres in terms of their architecture, cellular attachment ability and biodegradation.

4.1.1 Synthesis of smooth-walled (SW) microspheres

Emulsification/solvent-evaporation method was used for preparation of SW PLLA-EY microspheres according to the previous report (52). PLLA-EY was first dissolved in dichloromethane (DCM) at room temperature with a concentration of 2.0% (wt/v). This PLLA-EY solution was then slowly added drop-wise to 10-fold volume of PVA solution (2.0% (wt/v)) stirring at a speed of 300-600 rpm. The mixture was then continuously stirred overnight at room temperature. Once the DCM had evaporated completely, the resultant microspheres were sieved, washed with water, and finally freeze-dried. Microspheres in the size range of 20-60μm were used for further characterization.

4.1.2 Synthesis of nanofibrous (NF) microspheres

The NF microspheres were synthesized according to the protocol followed by Liu *et al*. (52). The PLLA-EY polymer was dissolved in tetrahydrofuran (THF) at 50°C in a concentration of 2.0% (wt/v). Under rigorous mechanical stirring at 500 rpm, glycerol (50°C) with 2.5 times the volume of the polymer-THF solution was gradually added into it, and stirred for 2-3 min afterwards. The mixture was then quickly poured into liquid nitrogen for flash freezing and

formation of nanofibers. After 10 min, a water-ice mixture (1L) was added for solvent exchange. The spheres were sieved, rinsed with distilled water, and finally freeze-dried. Microspheres in the size range of 20-60μm were sorted by sieving and used for further characterization.

4.2 METHOD FOR CHARACTERIZATION OF MICROSPHERES

4.2.1 Scanning electron microscopy (SEM)

The surface morphology and architecture of the microspheres was observed by SEM (JSM-6300). The freeze dried microspheres (20-60μm) were lightly sprinkled on the SEM stubs with a double sided adhesive carbon tape. The samples were first coated with gold (20mA, 50 mtorr) for 120 seconds and then analyzed under the SEM at 12-15 kV.

4.2.2 Confocal microscopy

The microspheres were analyzed for auto-fluorescence using a Leica SP5 confocal microscope equipped with an apochromatic 63x objective (0.9 N.A.). A small amount of sample was placed on a glass slide with a drop of oil or water and placed under the objective. The 514 nm Argon laser (~50% power) was used to excite the Eosin Y dye present in the polymer. Various z stacks and slices were acquired for the samples. The z-stacks were acquired for the entire depth of the microspheres (20-60 μm) and projected into 2D images. Multiple samples were analyzed for each type of polymer, and the images were taken.

4.2.3 *In vitro* cytotoxicity testing (MTS assay)

Cytotoxicity was assessed using 3-(4,5-dimethylthiazol-2-yl)-5-(3-carboxymethoxyphenyl)-2-(4-sulfophenyl)-2H-tetrazolium (MTS) assay. The aim was to determine if there are differences in cell viability between the dental pulp stem cells (DPSCs) cultured in presence/absence of PLLA-EY microspheres. The DPSCs (Passage 2) were a generous gift from Dr. Songtao Shi (University of Southern California, CA). These cells were allowed to proliferate to passage 5 and were seeded on 96-well tissue culture polystyrene (TCPS)

plates at a density of 6000 cells/well (3000 cells for 21d) for 24 hrs. Microspheres (SW and NF) from PLLA-EY 200:1 were pretreated with alcohol for an hour and washed twice in PBS before adding them to the cells in the wells, with a density of 1000 microspheres per well. Cells cultured without microspheres served as controls. Thus 6 groups were formed- NF-MS, SW-MS, NF-Cells, SW-Cells, Cells (DPSC) only and culture medium.

The microplates were cultured in α-MEM supplemented with 10% fetal bovine serum (FBS) containing 1% Pen-Strept antibiotics (Gibco, USA). They were kept on a plate shaker (50 rpm) under humid atmosphere at 37°C with 5.0% CO_2 for 1, 3, 7 and 21 days. Triplicates were used for each group. The media was changed every other day. The cell viability was assessed using a MTS assay kit (CellTiter 96® Aqueous One Solution Cell Proliferation Assay, Promega, Madison, WI, USA). For this assay, the media was replaced by 1ml of fresh media and to this, 200 µl MTS solution was added, this was incubated in a cell-culture incubator for 2.5 hrs. The absorbance was measured at 490 nm using a 96-well microplate reader. The absorbance of the microspheres only group (NF and SW) was subtracted from their respective microsphere-cell group (NF-Cells, SW-Cells) to omit any effects the Eosin Y dye might cause on the absorbance. The cell viability was normalized against the culture of 1 day DPSCs. Statistical analysis was done to determine if significant differences existed between the 3 groups (NF-Cells, SW-Cells, Cells only) at each time point by one way ANOVA. P-value of < 0.05 was considered to be statistically significant.

The light microscopy images of the 21 day samples were taken at various magnifications with a camera attached to the microscope.

4.2.4 Biodegradation of microspheres

The biodegradation of microspheres was tested *in vitro* for PLLA-EY 400:1 polymer. Two groups were formed- NF-MS and SW-MS. These were analyzed for biodegradation at three

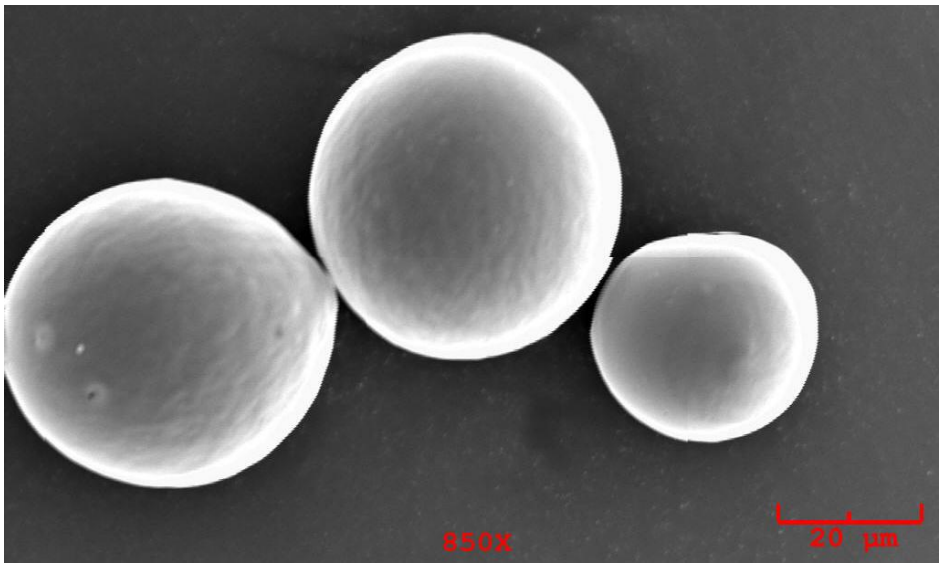

Figure 7. SEM images for SW microspheres prepared with PLLA-EY 200:1

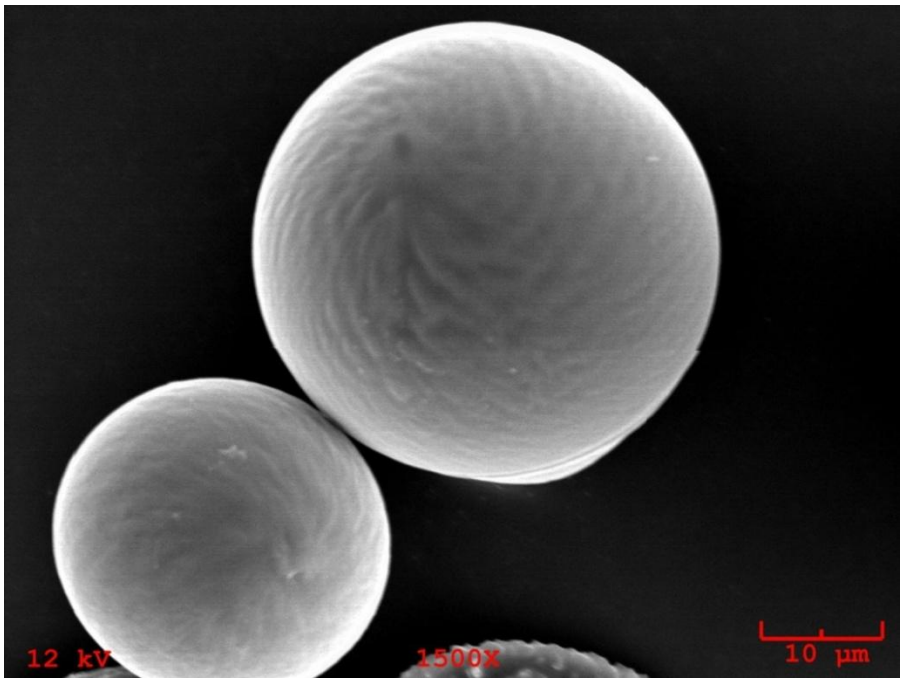

Figure 8. SEM images for SW microspheres prepared with PLLA-EY 400:1

time points- 1wk, 3 wk and 6 wks.

About 15 mg of microspheres from each group were placed per vial in the 1 ml plastic vials and to this; 1 ml of PBS solution (0.01 M, pH 7.4) was added. Triplicates were prepared for each time point. The PBS was changed every 3 days, and the supernatant was collected for testing the pH every 3 days initially and then every week thereafter. At 1, 3 and 6 weeks, the microsphere samples were taken out. These were rinsed with deionized water and freeze dried. The SEM images were taken with the method described before.

4.3 RESULTS

4.3.1 Scanning electron microscopy (SEM)

SEM images for SW microspheres prepared with PLLA-EY 200:1 and PLLA-EY 400:1 are shown in Figures 7 and 8. Both the polymers formed microspheres that were spherical, smooth walled and most of the microspheres were in the desirable size range of 20-60μm. No differences were seen between the polymers in terms of surface smoothness and architecture of the microspheres.

NF microspheres prepared with PLLA-EY 200:1 shows that it was able to form microspheres in which nanofibrous architecture was just beginning for form (Figure 9A). The surface of the microsphere was highly porous but distinct nanofibers were not seen (Figure 9B). In comparison to this, the PLLA EY 400:1 formed microspheres with well-defined and nanofibrous architecture, as seen in Figure 10(A, B).

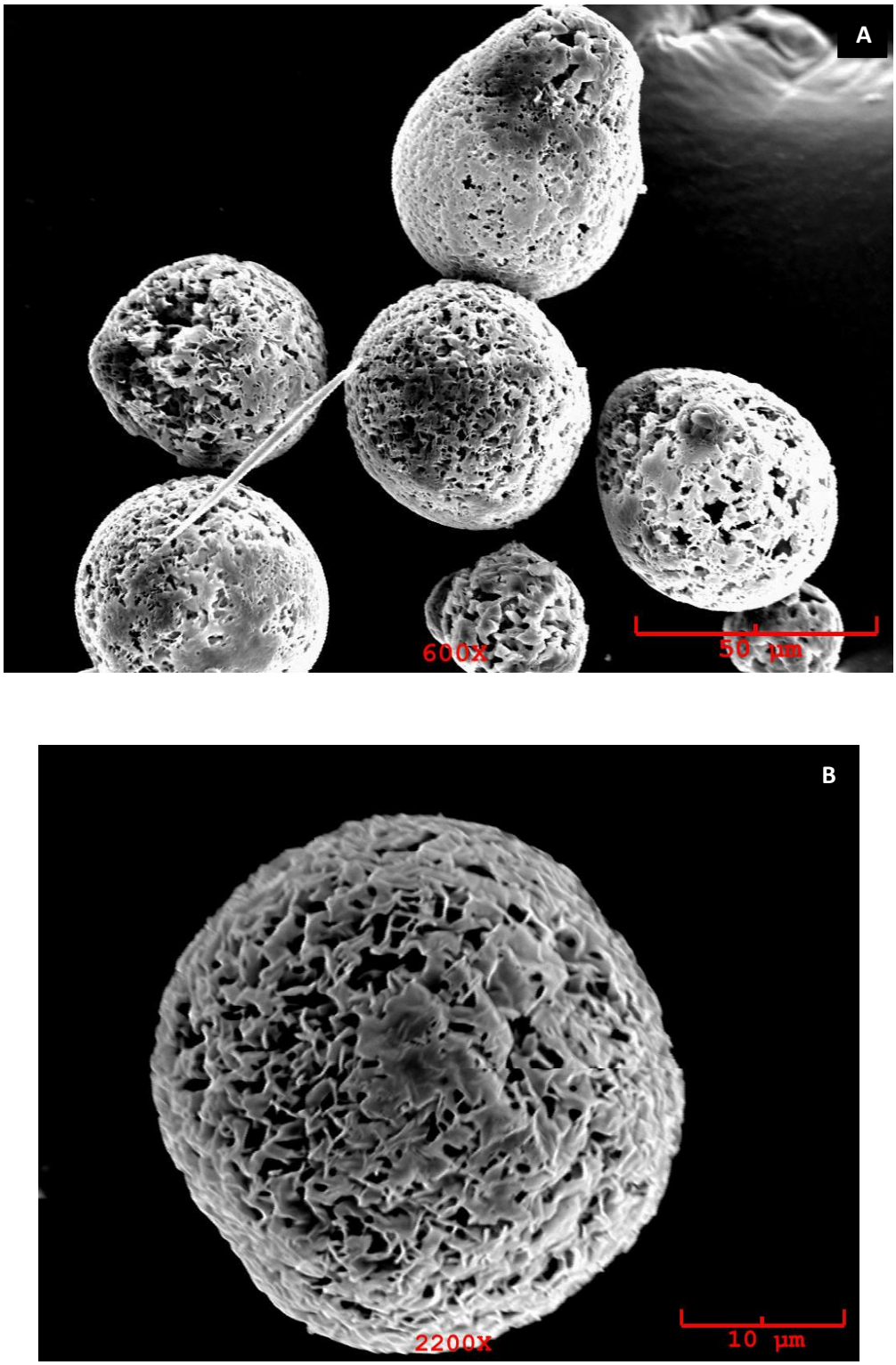

Figure 9. A) SEM images for NF microspheres prepared with PLLA-EY 200:1; B) SEM image of a single NF microsphere prepared with PLLA-EY 200:1

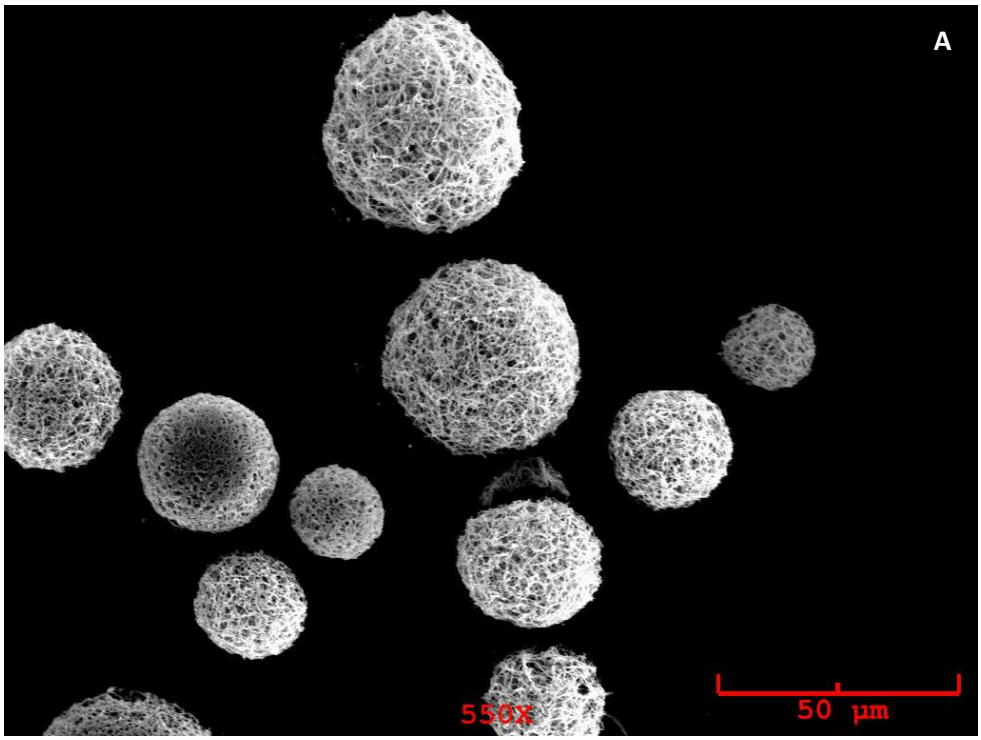

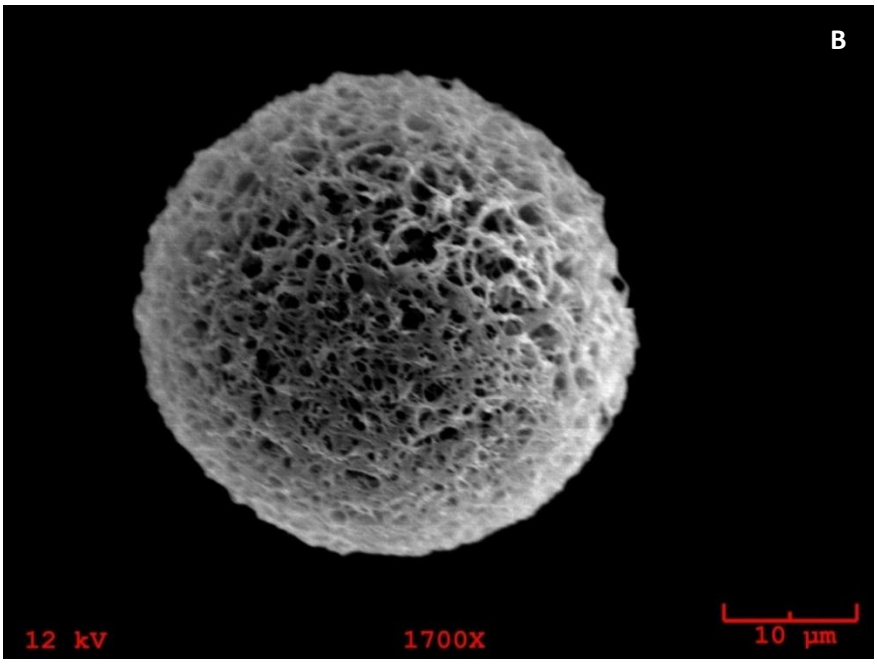

Figure 10. A) SEM images for NF microspheres prepared with PLLA-EY 400:1; B) SEM image of a single NF microsphere prepared with PLLA-EY 400:1

4.3.2 Confocal microscopy

The confocal images of SW microspheres prepared with PLLA-EY 200:1 and PLLA-EY 400:1 are shown in Figures 11 and 12, respectively. From the images, it can be seen that the microspheres are auto-fluorescent and the fluorescence is in the emission range of EY, indicating that EY has incorporated into the PLLA polymer. No differences are seen in the SW microspheres from both the polymers.

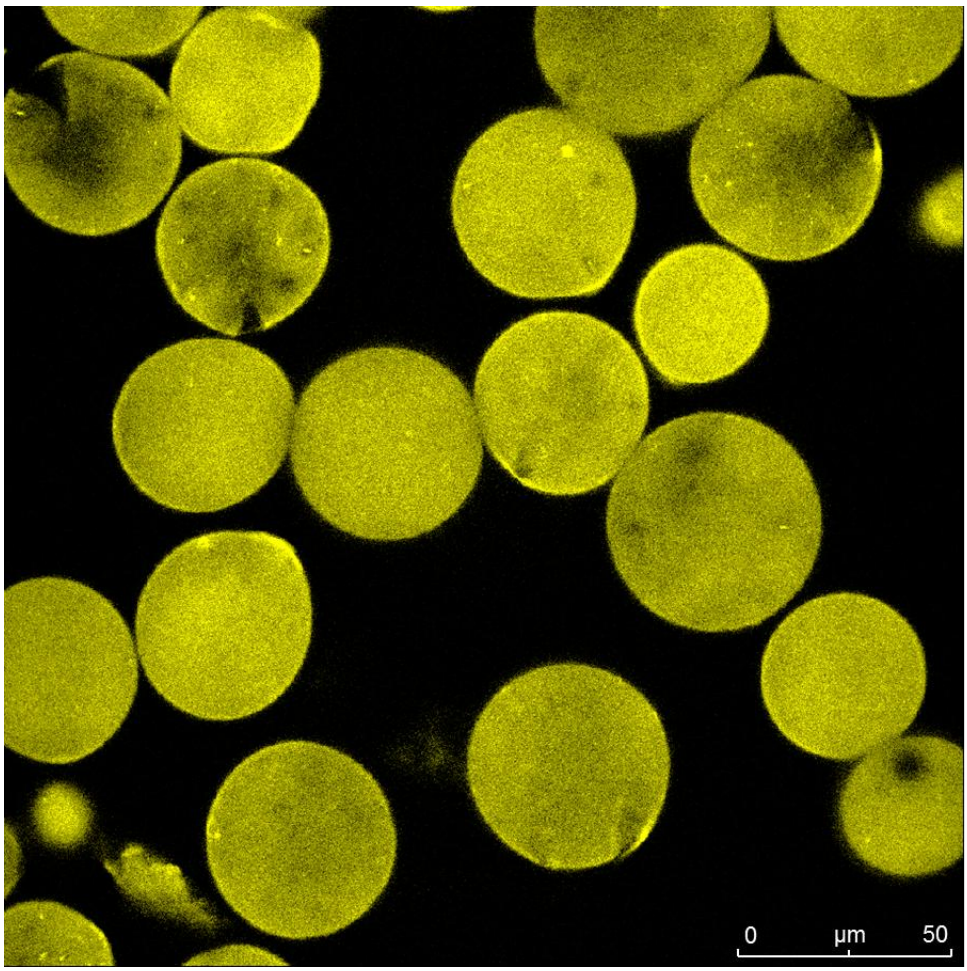

Figure 11. Confocal image of smooth walled microspheres prepared with PLLA-EY 200:1

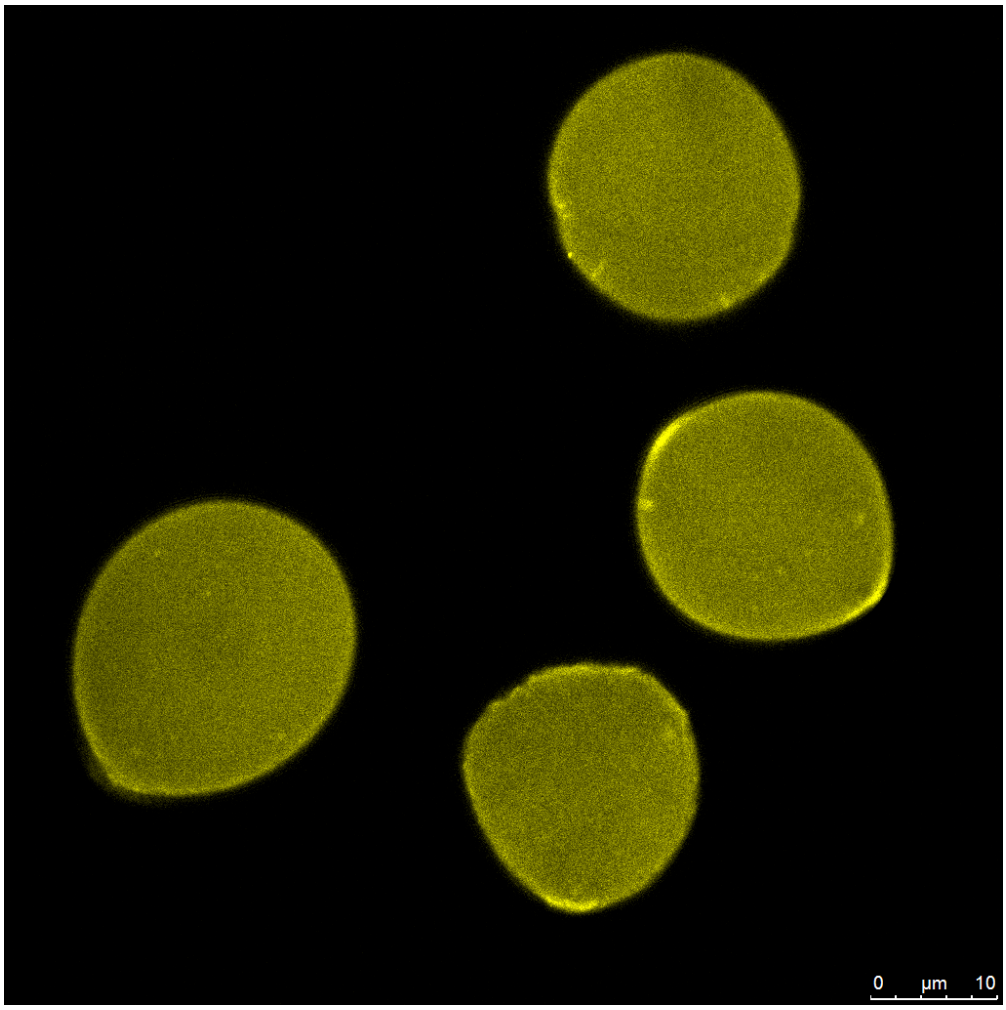

Figure 12. Confocal image of smooth walled microspheres prepared with PLLA-EY 400:1

The confocal images of NF microspheres prepared with PLLA-EY 200:1 and PLLA-EY 400:1 are shown in Figures 13 and 14, respectively. It can be seen that the microspheres are auto-fluorescent and the fluorescence is in the emission range of EY, indicating that EY has incorporated into the PLLA polymer. On comparing both the polymers, the outer boundary of microspheres prepared from PLLA-EY 400:1 appears more porous and ragged, and the microsphere surface is more intricate, indicating a more nanofibrous architecture compared to the PLLA-EY 200:1.

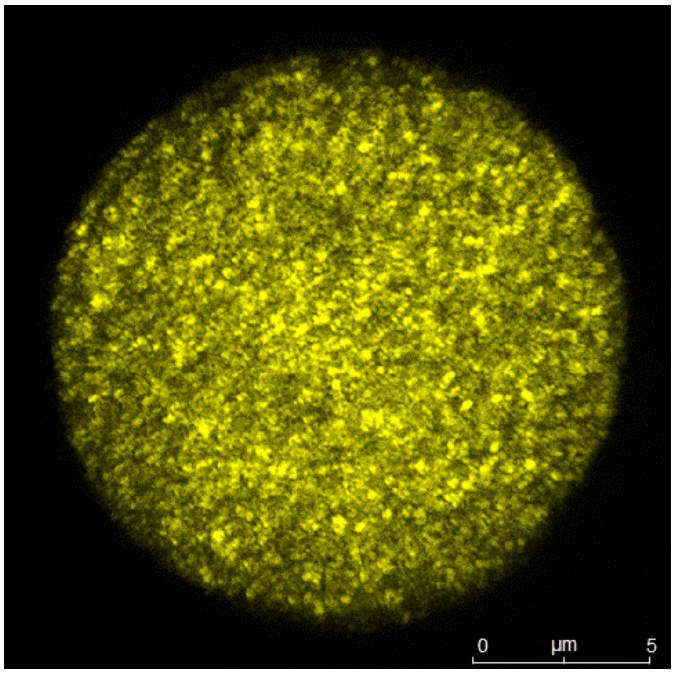

Figure 13. Confocal image of a single nanofibrous microsphere prepared with PLLA-EY 200:1

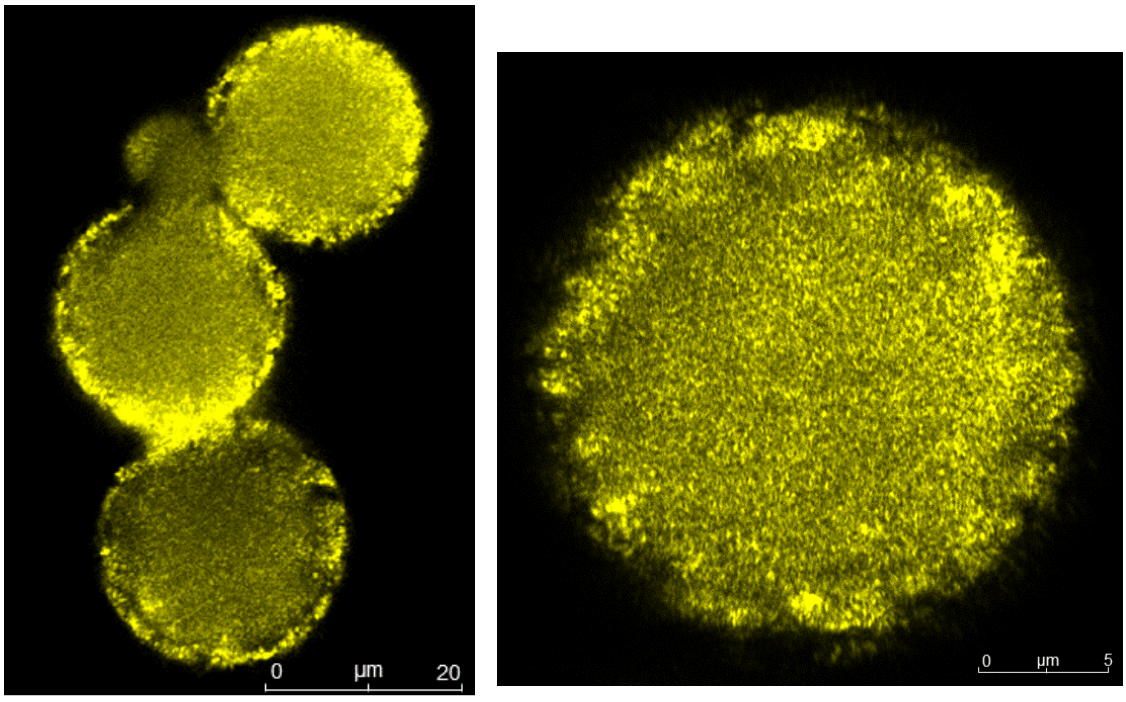

Figure 14. Confocal images of nanofibrous microspheres prepared with PLLA-EY 400:1

4.3.3 *In vitro* cytotoxicity testing (MTS assay)

Cells continue to proliferate even in presence of PLLA-EY microspheres (Figure 15). At day 3, the number of cells increases two-fold compared to day 1. At day 7, there is a 4.5 fold increase in cell number, and this continues to a 7-8 fold increase at day 21. At day 21, the cell viability in the presence of NF microspheres (NF-cell group) and SW microspheres (SW-cell group) is higher than the DPSC only group. This indicates that the presence of microspheres around the cells supported cell growth. The cell viability in the NF group was more than in the SW group; this supports the idea that NF microspheres provide a more biomimetic 3D environment for cell growth, as has been shown in previous studies.

The percent cell viability at day 7 and day 21 for the both the microsphere containing groups were higher than the cell only group. Also, at day 21, the NF-cell group had higher viability values compared to the SW group indicating a higher growth of cells on the NF microspheres compared to the SW microspheres. However, no significant differences were seen in the cell viability values at day 1 (ANOVA, $p=0.054$), day 3 (ANOVA, $p=0.08$), day 7 (ANOVA, $p=0.63$) and day 21 (ANOVA, $p=0.12$).

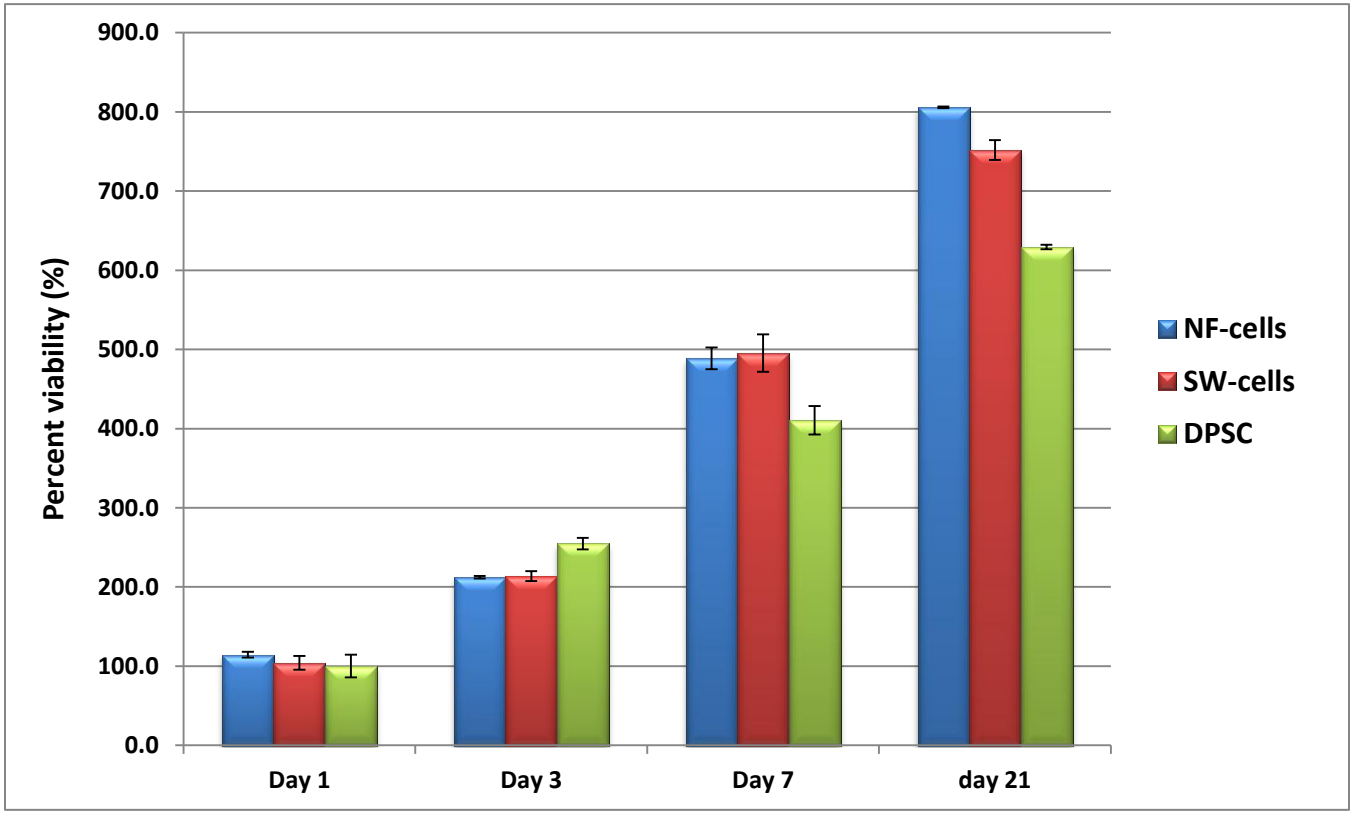

Figure 15. Percent viability graph of DPSCs determined from the MTS cytotoxicity assay. Error bars indicate standard deviations

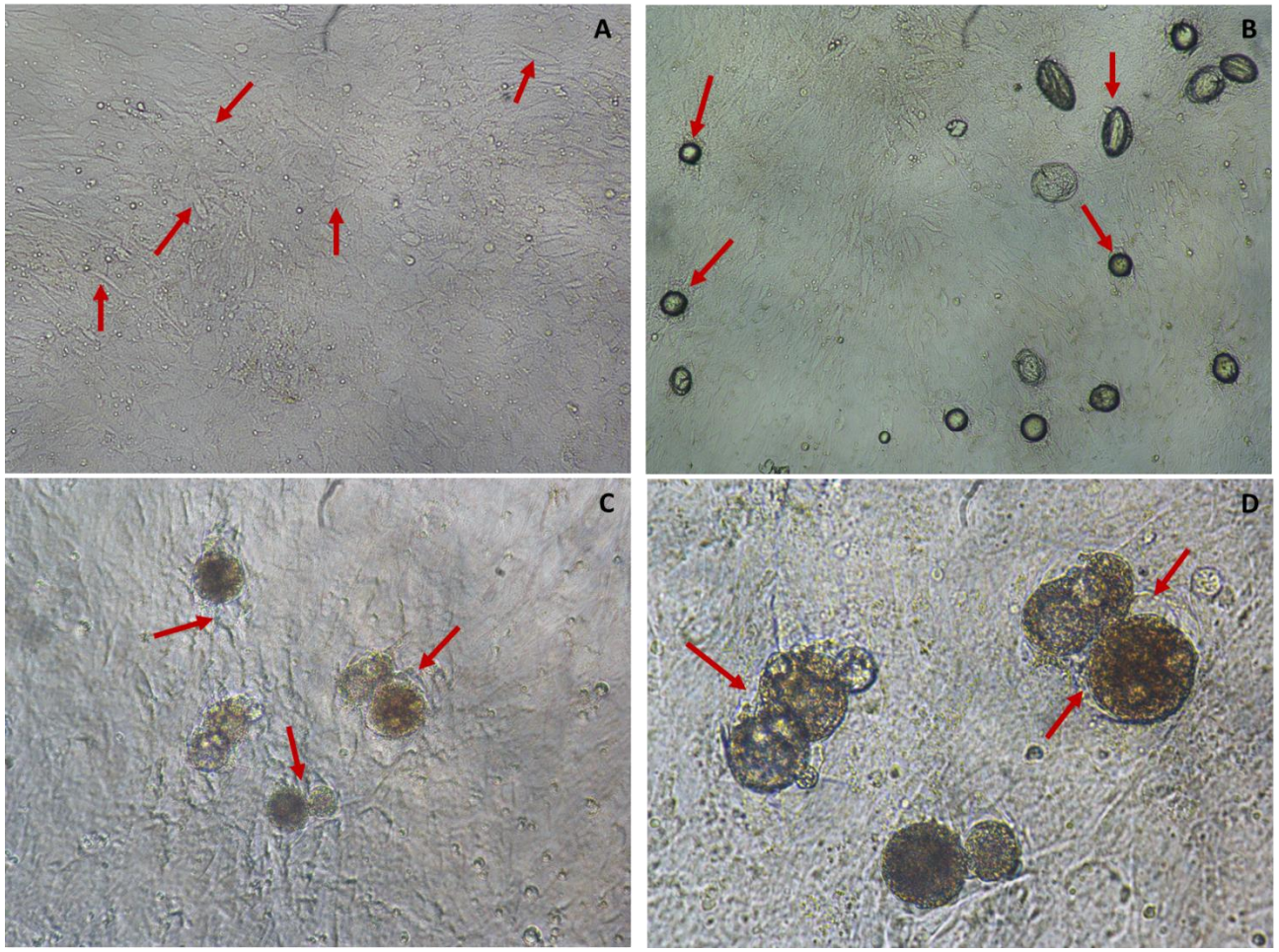

Figure 16. Light microscopy images of MTS assay of PLLA EY 200:1 at day 21. Red arrows indicate DPSCs A) DPSC only (20x); B) Cells attached around SW microspheres (20x); C) Cells attached to NF microspheres (20x); D) Higher magnification of C (40X) showing aggregated microspheres and cell attachment on them

The light microscopy images of the MTS assay (day 21) are seen in Figure 16. The cells are attached on microsphere surface (both SW and NF) in the microsphere-cell group. Most NF microspheres formed aggregates due to cell adhesion around and between the microspheres (Figure 16 C, D), something which was not observed in the SW group (Figure 16B).

4.3.4 Biodegradation of microspheres

No change in pH values was seen in the supernatant solutions collected from the biodegradation study. No differences were seen in the pH values between SW and NF microspheres (Figure 17). Around day 70 however, it was observed that the pH values of NF microspheres slightly decreased as compared to the SW microspheres.

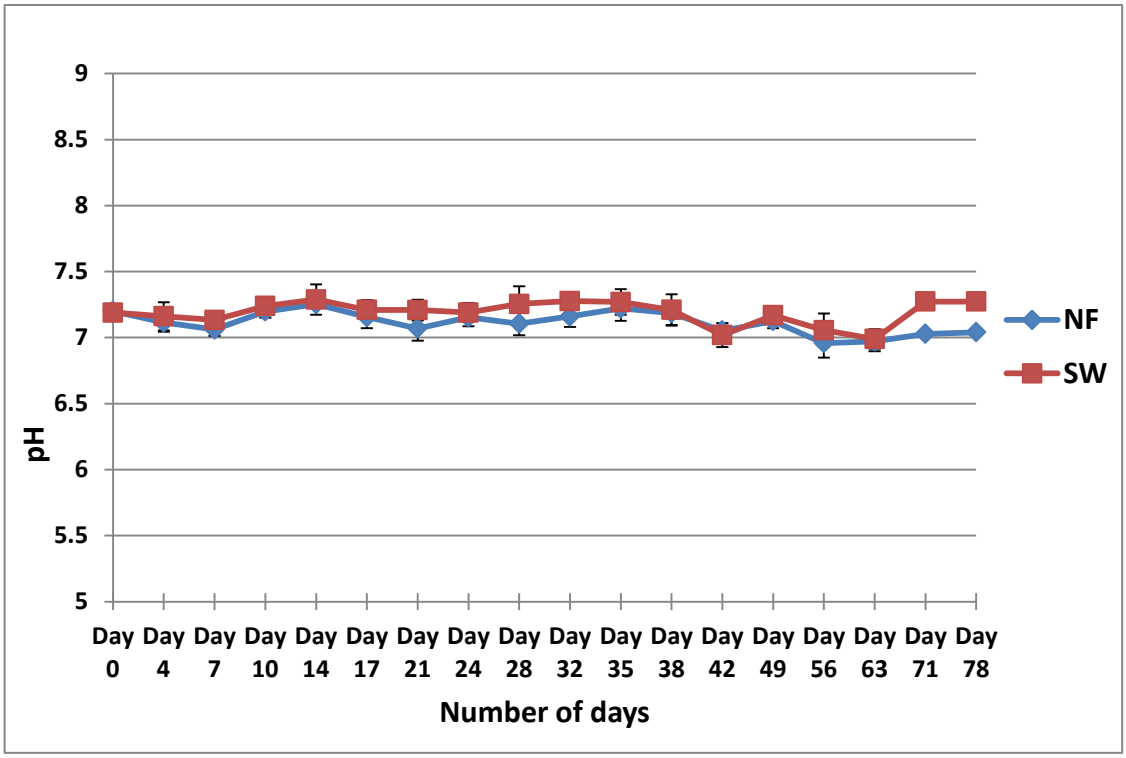

Figure 17.pH values of PBS samples collected from *in vitro* biodegradation of NF and SW microspheres

The SEM images of SW microspheres collected from biodegradation experiment are shown in Figure 18. No differences were seen in the microspheres incubated for 1, 3 weeks (Figure 18A,B) and 6 weeks, indicating that the disintegration of microspheres had not started even at the end of 6 weeks immersion in PBS solution (Figure 18C).

The SEM images of NF microspheres collected from biodegradation experiment are shown in Figure 19. There was no change in the microspheres incubated for 1 week and 3 weeks

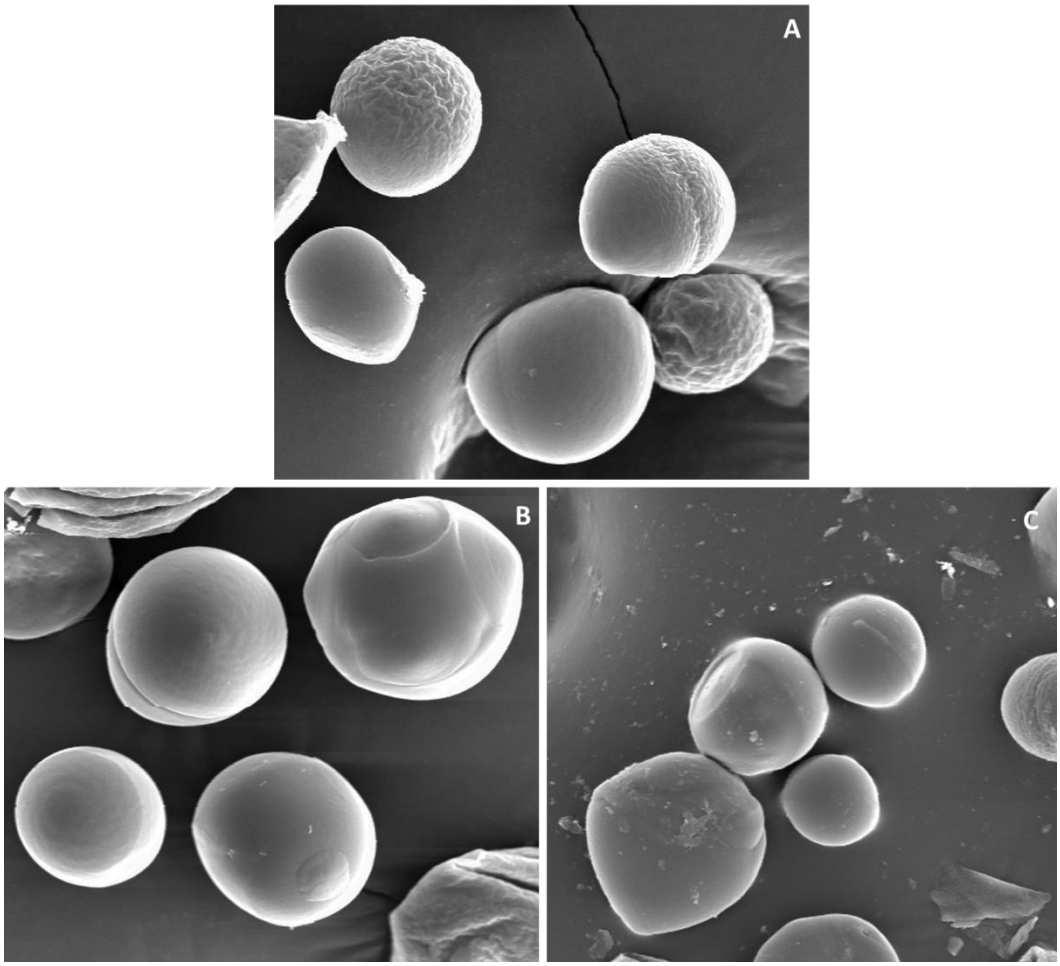

Figure 18. SEM images of biodegradation of SW microspheres incubated in PBS solution for A) 1 wk; B) 3 wks; C) 6 wks

(Figure 19A, B), but at 6 weeks of incubation in PBS solution, some microspheres retained their original spherical shape while in some areas, microsphere disintegration was seen with broken down microspheres and debris in the vicinity (indicated by red arrows in Figure 19C), indicating that the biodegradation process had started taking place in the NF microspheres.

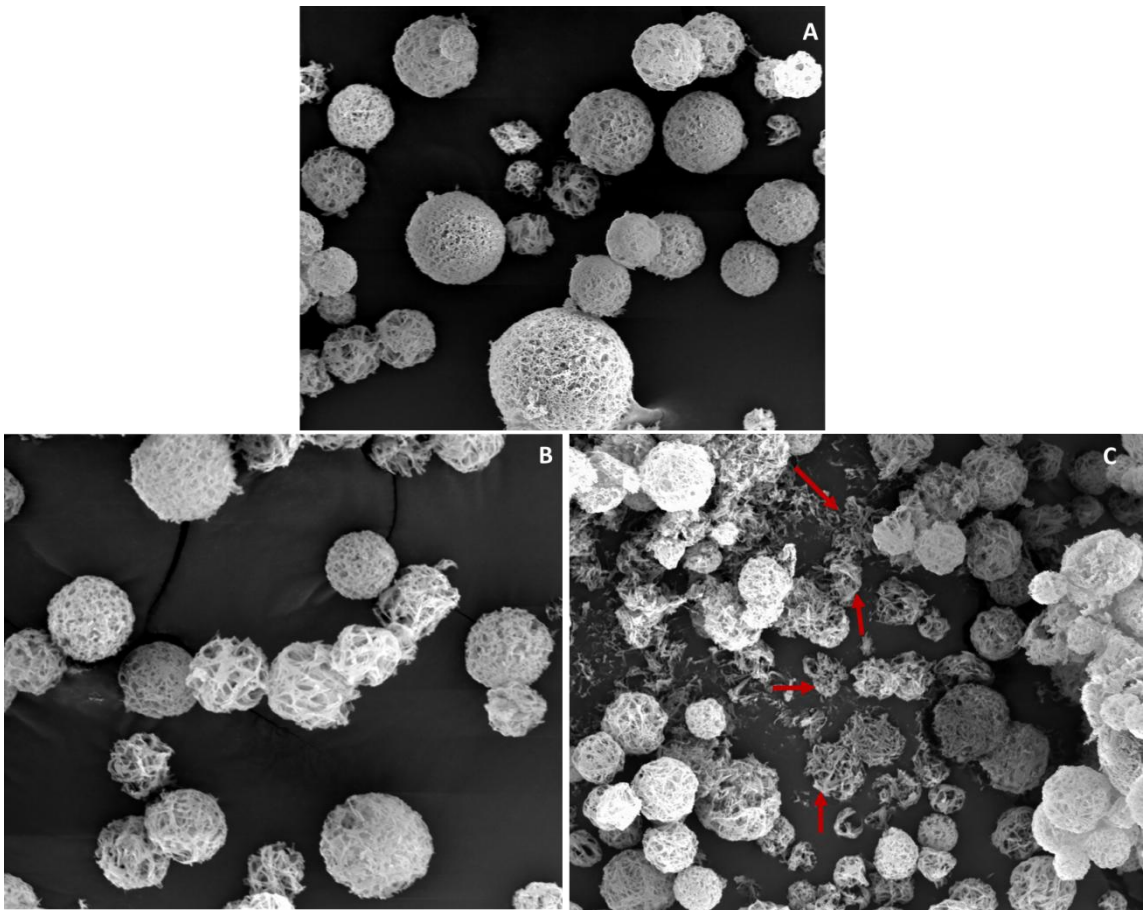

Figure 19. SEM images of biodegradation of NF microspheres incubated in PBS solution for A) 1 wk; B) 3 wks; C) 6 wks. Red arrows indicates debris from microsphere biodegradation

4.4 DISCUSSION

The second aim of the current study was to synthesize microspheres from the fluorescent PLLA-EY polymer described in the previous chapter. Two polymers were used for microsphere synthesis- PLLA-EY 200:1 and 400:1. It is important to note that the molecular weights of polymers PLLA-EY 20:1 and 100:1 were too low to be able to form microspheres. Also, higher initiator content might mean greater cytotoxic effects, which we wanted to optimize. It has been observed that the appropriate size of microspheres for injectability for clinical use is about 25-60μm, so further characterization of microspheres was done using microspheres of this size range.

A thermally induced phase separation technique (TIPS) that has been described previously (156-159) and used for microparticle synthesis by Liu *et al.* (52), was used for synthesis of microspheres. The TIPS is a liquid-liquid phase separation technique developed by Ma *et al* (157). This technique yields PLLA matrix with fiber length ranging from 50-500nm and involves polymer dissolution, phase separation and solvent exchange, freezing and freeze-drying (160, 161). In context with the current study, the PLLA-EY was first dissolved in THF solvent. Addition of glycerol to this mixture while stirring vigorously led to phase separation and formation of a polymer rich phase formed from PLLA-EY microspheres and a polymer lean phase formed by the solvent, as described previously (162). The speed of the mechanical stirrer was optimized to obtain a higher yield in the desirable size range. Rapid pouring of this mixture into liquid N_2 caused flash freezing with formation of nanofibrous architecture in the microspheres (157). The solvents were exchanged with water-ice mixture and then the microspheres were freeze-dried. These NF scaffolds are highly desirable in tissue engineering since they mimic the physical architecture of natural extracellular matrix (ECM) and are highly superior to SW scaffolds in promoting cell migration, attachment, proliferation and

differentiation for tissue engineering (163-165). The additional benefit of using nanofibrous microspheres in tissue engineering is that they are also injectable owing to their micron size.

Differences in architecture were seen between nanofibrous microspheres synthesized from PLLA-EY 200:1 and 400:1 by SEM and confocal microscopy. The 400:1 polymer formed highly well-defined nanofibers, similar to those formed by PLLA in previous studies (116, 157). However, in the 200:1 polymer, the nanofibers were partially formed or just starting to form. These differences can be explained by the different molecular weights of the two polymers with PLLA-EY 400:1 being of higher molecular weight. According to the principle of nanofibers formation, the molecular weight of a polymer is an indicator of the polymer chain entanglement in the solution. At the same polymer concentration, lowering the molecular weight causes formation of beaded structures while increasing the molecular weight tends to form smooth fibers (166). Thus, an increase in molecular weight of the polymer is associated with formation of more well defined nanofibers, as seen in the 400:1 polymer. Microspheres were also attempted to be synthesized from the 100:1 polymer but microspheres could not be formed due to its very low molecular weight.

The MTS assay for cell viability tested the cytotoxicity of EY on DPSCs. The microspheres from PLLA-EY 200:1 were used, since this polymer incorporated more initiator than the 400:1 polymer. The microspheres were first pretreated with alcohol for pre-wetting and washed twice in PBS before they were mixed with the cells. For the 21 day culture, number of seeded cells were reduced to half compared to other groups, because long term culture with more cells could cause cell death from over-confluence or insufficient nutrition which could be confused with cell death caused by EY. The results showed that at day 21 in culture, the percent viability of DPSCs for the NF-cell group > SW-cell group > DPSC only group. Also, in the NF-cell group, small aggregates of microspheres were formed, with cellular processes of DPSCs

extending between the adjacent cells and microspheres. These findings resulted from the higher surface area of nanofibrous architecture, which favors cellular adhesion, proliferation, migration and differentiation (164, 165, 167, 168). It would be interesting to evaluate the cell migration and ell-cell and cell-scaffold interaction on the scaffolds by evaluating gene expression.

Biodegradation is an important property of the scaffolding material that needs consideration in tissue engineering. Ideally, a scaffold should disintegrate at the right rate to match the new tissue formation. The biodegradation process of PLLA involves hydrolytic attack of the ester bond with formation of lactic acid and an alcohol. The biodegradation properties are affected by a variety of intrinsic and local factors like crystallinity, molecular weight, polymer concentration, hydrophobicity, temperature, presence of enzymes etc (169-171). In the presence of water, the polymer rapidly plasticizes and ultimately leads to mechanical distortion and fracture of the polymer. One way to characterize the degradation of PLLA is by measuring the pH since lactic acid is released upon its degradation. Also, because of the porous architecture the NF microspheres are expected to degrade faster than SW microspheres. In the current study, not much difference was seen in the pH between the two groups. However, the SEM images showed that the biodegradation of NF PLLA-EY microspheres had started by 6 weeks *in vitro*, whereas no biodegradation was seen in the SW PLLA-EY microspheres. This time point should be suitable for the microspheres to be used for application of pulp tissue regeneration. However, the factors that cause biodegradation *in vivo* are very different than *in vitro* and evaluating the biodegradation process *in vivo* needs to be a part of future research.

Future studies are needed to evaluate the cell adhesion, proliferation and differentiation of DPSCs by gene expression on these fluorescent microsphere scaffolds. It would also be interesting to inject these microspheres *in vivo* with the DPSCs and evaluate the newly tissue formed histologically and immunologically.

5. CONCLUSIONS

Based on the data and observations from the study, we can conclude that we were able to synthesize an auto-fluorescent PLLA-EY polymer by a ring opening polymerization process, using Eosin Y as a fluorescent initiator. The presence of fluorescent initiator in the polymer was confirmed by FT-IR where the peaks generated from Eosin Y were observed in the fluorescent polymer. UV-visible spectrometry also confirmed the presence of absorbance peak from Eosin Y in the PLLA-EY polymer at around 530nm.

The microspheres were fabricated from the PLLA-EY polymer and were found to be auto-fluorescent under confocal microscopy. The florescence was in the emission range of EY, indicating the incorporation of EY in the polymer.

Another finding was that as the M/I molar ratio was increased, an increase in the molecular weight of the polymer was observed. Also, the nanofibrous architecture changed with more well-defined nanofibers being formed with the higher molecular weight PLLA-EY 400:1 polymer, as compared to the lower molecular weight PLLA-EY 200:1.

Both short term (7d) and long term (21d) *in vitro* cytotoxicity results from the MTS assay confirmed that the fluorescent polymer was non-toxic to the DPSCs. It was interesting to see under light microscope, the formation of aggregates of NF microspheres that were held together by cellular extensions of DPSCs. The data also confirmed that the NF architecture was superior to the SW surface for cell growth, an observation that has been made in previous studies. The presence of EY did not appear to alter cellular response to the microparticles.

Biodegradation of the NF microspheres was not seen until 6 weeks *in vitro* in PBS solution under the SEM, whereas no biodegradation was observed in SW microspheres even at 6 weeks incubation.

Based on this data, the polymer should be useful for tissue engineering. Future studies are needed to determine the cell-microsphere interaction including cell adhesion, proliferation, differentiation, as well as and placement of the microspheres *in vivo* with the DPSCs to evaluate the *de novo* tissue formation.

REFERENCES

1. Olympus America Inc. 2012 . Microscopy resource center- Fluorescence microscopy; Retrieved from http://www.olympusmicro.com/primer/techniques/fluorescence/fluorhome.html

2. Langer R, Vacanti J. Tissue engineering. Science. 1993;260(5110):920-6.

3. Kulmala S, Suomi J. Current status of modern analytical luminescence methods. Analytica Chimica Acta. 2003;500(1–2):21-69.

4. Resch-Genger U, Grabolle M, Cavaliere-Jaricot S, Nitschke R, Nann T. Quantum dots versus organic dyes as fluorescent labels. Nat Methods. 2008;5(9):763-75.

5. Zhang J, Campbell RE, Ting AY, Tsien RY. Creating new fluorescent probes for cell biology. Nat Rev Mol Cell Biol. 2002;3(12):906-18.

6. Waggoner A. Fluorescent labels for proteomics and genomics. Curr Opin Chem Biol. 2006;10(1):62-6.

7. Wang F, Tan WB, Zhang Y, Fan XP, Wang MQ. Luminescent nanomaterials for biological labelling. Nanotechnology. 2006;17(1):R1-R13.

8. Lavis LD, Raines RT. Bright ideas for chemical biology. ACS Chem Biol. 2008;3(3):142-55. PMCID: 2802578.

9. Shimomura O, Johnson FH, Saiga Y. Extraction, purification and properties of Aequorin, a bioluminescent protein from the luminous hydromedusan, Aequorea. J Cell Comp Physiol. 1962;59(3):223-39.

10. Shimomura O. Discovery of Green Fluorescent Protein. Green Fluorescent Protein: John Wiley & Sons, Inc. NY ; 2005. p. 1-13.

11. Gerdes H-H, Kaether C. Green fluorescent protein: applications in cell biology. Febs Letters. 1996;389(1):44-7.

12. Misteli T, Spector DL. Applications of the green fluorescent protein in cell biology and biotechnology. Nat Biotechnol. 1997;15(10):961-4.

13. Heim R, Tsien RY. Engineering green fluorescent protein for improved brightness, longer wavelengths and fluorescence resonance energy transfer. Curr Biol. 1996;6(2):178-82.

14. Michalet X, Pinaud FF, Bentolila LA, Tsay JM, Doose S, Li JJ, *et al*. Quantum dots for live cells, in vivo imaging, and diagnostics. Science. 2005;307(5709):538-44.

15. Mauring K, Krasnenko V, Miller S. Photophysics of the blue fluorescent protein. J. Lumin.122-123(0):291-3.

16. Glazer AN, Fang S. Chromophore content of blue-green algal phycobiliproteins. J Biol. Chem. 1973;248(2):659-62.

17. Oi VT, Glazer AN, Stryer L. Fluorescent phycobiliprotein conjugates for analyses of cells and molecules. J Cell Biol. 1982;93(3):981-6. PMCID: 2112146.

18. Glazer A. Phycobiliproteins- a family of valuable, widely used fluorophores. J Appl Phycol. 1994;6(2):105-12.

19. Polysciences, Inc. 2014. Microspheres & Particles Handling Guide. Retrieved from http://www.polysciences.com/SiteData/docs/Microparti/dbdc94c1bcbdf576/Microparticles%20Guide.pdf

20. Schluchter W, Glazer A. Biosynthesis of phycobiliproteins in cyanobacteria. In: Peschek G, Löffelhardt W, Schmetterer G, editors. The phototrophic prokaryotes: Springer US; 1999. p. 83-95.

21. Matsumoto K, Nojima T, Sano H, Majima K. Fluorescent lanthanide chelates for biological systems. Macromol Symp. 2002;186(1):117-21.

22. Xiao M, Selvin PR. Quantum yields of luminescent lanthanide chelates and far-red dyes measured by resonance energy transfer. J Am Chem Soc. 2001;123(29):7067-73.

23. Soini EJ, Pelliniemi LJ, Hemmila IA, Mukkala VM, Kankare JJ, Frojdman K. Lanthanide chelates as new fluorochrome labels for cytochemistry. J Histochem Cytochem. 1988;36(11):1449-51.

24. Ray SC, Saha A, Jana NR, Sarkar R. Fluorescent carbon nanoparticles: Synthesis, Characterization, and Bioimaging Application. J. Phys. Chem. C. 2009;113(43):18546-51.

25. Bhunia SK, Saha A, Maity AR, Ray SC, Jana NR. Carbon nanoparticle-based fluorescent bioimaging probes. Sci Rep. 2013;3:1473. PMCID: 3600594.

26. Ow H, Larson DR, Srivastava M, Baird BA, Webb WW, Wiesner U. Bright and stable core-shell fluorescent silica nanoparticles. Nano Lett. 2005;5(1):113-7.

27. Burns A, Ow H, Wiesner U. Fluorescent core-shell silica nanoparticles: towards "Lab on a Particle" architectures for nanobiotechnology. Chem Soc Rev 2006;35(11):1028-42.

28. Santra S. Fluorescent silica nanoparticles for cancer imaging. Methods Mol Biol. 2010;624:151-62.

29. Chan WCW, Maxwell DJ, Gao X, Bailey RE, Han M, Nie S. Luminescent quantum dots for multiplexed biological detection and imaging. Curr Opin Biotech. 2002;13(1):40-6.

30. Alivisatos AP, Gu W, Larabell C. Quantum dots as cellular probes. Annu Rev Biomed Eng. 2005;7:55-76.

31. Gao X, Yang L, Petros JA, Marshall FF, Simons JW, Nie S. *In vivo* molecular and cellular imaging with quantum dots. Curr Opin Biotech. 2005;16(1):63-72.

32. Kairdolf BA, Smith AM, Stokes TH, Wang MD, Young AN, Nie S. Semiconductor quantum dots for bioimaging and biodiagnostic applications. Annu Rev Anal Chem 2013;6(1):143-62.

33. Jamieson T, Bakhshi R, Petrova D, Pocock R, Imani M, Seifalian AM. Biological applications of quantum dots. Biomaterials. 2007;28(31):4717-32.

34. Rosenthal SJ, Chang JC, Kovtun O, McBride JR, Tomlinson ID. Biocompatible quantum dots for biological applications. Chem Biol. 2011;18(1):10-24.

35. Derfus AM, Chan WCW, Bhatia SN. Probing the Cytotoxicity of semiconductor quantum dots. Nano Letters. 2003;4(1):11-8.

36. Kirchner C, Liedl T, Kudera S, Pellegrino T, Muñoz Javier A, Gaub HE, *et al.* Cytotoxicity of colloidal CdSe and CdSe/ZnS nanoparticles. Nano Letters. 2004;5(2):331-8.

37. Hezinger AFE, Teßmar J, Göpferich A. Polymer coating of quantum dots – A powerful tool toward diagnostics and sensorics. Eur. J. Pharm. Biopharm. 2008;68(1):138-52.

38. Su Y, He Y, Lu H, Sai L, Li Q, Li W, *et al*. The cytotoxicity of cadmium based, aqueous phase – Synthesized, quantum dots and its modulation by surface coating. Biomaterials. 2009;30(1):19-25.

39. Nida DL, Nitin N, Yu WW, Colvin VL, Richards-Kortum R. Photostability of quantum dots with amphiphilic polymer-based passivation strategies. Nanotechnology. 2008;19(3).

40. Qiu LY, Bae YH. Self-assembled polyethylenimine-graft-poly(epsilon-caprolactone) micelles as potential dual carriers of genes and anticancer drugs. Biomaterials. 2007;28(28):4132-42. PMCID: 2691394.

41. Zhang Y, Yang J. Design strategies for fluorescent biodegradable polymeric biomaterials. J Mater Chem B Mater Biol Med. 2013;1(2):132-48. PMCID: 3660738.

42. Oh W-K, Jeong YS, Song J, Jang J. Fluorescent europium-modified polymer nanoparticles for rapid and sensitive anthrax sensors. Biosens. Bioelectron. 2011;29(1):172-7.

43. Acosta MA, Ymele-Leki P, Kostov YV, Leach JB. Fluorescent microparticles for sensing cell microenvironment oxygen levels within 3D scaffolds. Biomaterials. 2009;30(17):3068-74.

44. Brown JQ, Srivastava R, McShane MJ. Encapsulation of glucose oxidase and an oxygen-quenched fluorophore in polyelectrolyte-coated calcium alginate microspheres as optical glucose sensor systems. Biosens. Bioelectron. 2005;21(1):212-6.

45. Disney MD, Zheng J, Swager TM, Seeberger PH. Detection of bacteria with carbohydrate-functionalized fluorescent polymers. J. Am. Chem. Soc. 2004;126(41):13343-6.

46. Kumar V, Adamson DH, Prud'homme RK. Fluorescent Polymeric Nanoparticles: Aggregation and Phase Behavior of Pyrene and Amphotericin B Molecules in Nanoparticle Cores. Small. 2010;6(24):2907-14.

47. Liu Y, Wu J, Meng L, Zhang L, Lu X. Self-assembled, fluorescent polymeric micelles of a graft copolymer containing carbazole for thermo-controlled drug delivery *in vitro.* J. Biomed. Mater. Res. Part B Appl. Biomater. 2008;85B(2):435-43.

48. Feng X, Lv F, Liu L, Tang H, Xing C, Yang Q, *et al*. Conjugated polymer nanoparticles for drug delivery and imaging. ACS Appl Mater Interfaces. 2010;2(8):2429-35.

49. Wu C, Bull B, Szymanski C, Christensen K, McNeill J. Multicolor conjugated polymer dots for biological fluorescence imaging. ACS Nano. 2008;2(11):2415-23.

50. Zhang G, St. Clair TL, Fraser CL. Synthesis and fluorescent properties of difluoroboron dibenzoylmethane polycaprolactone. Macromol. 2009;42(8):3092-7.

51. Hou Q, De Bank PA, Shakesheff KM. Injectable scaffolds for tissue regeneration. J. Mater. Chem. 2004;14(13):1915-23.

52. Liu X, Jin X, Ma PX. Nanofibrous hollow microspheres self-assembled from star-shaped polymers as injectable cell carriers for knee repair. Nat Mater. 2011;10(5):398-406.

53. Sun-Woong Kang OJ, Byung-Soo Kim. PLGA microspheres as an injectable scaffold for cartilage tissue engineering. Tissue Eng. 2005;11(3-4):438-47.

54. Huang S, Fu X. Naturally derived materials-based cell and drug delivery systems in skin regeneration. J. Control. Release 2010;142(2):149-59.

55. Mano JF, Silva GA, Azevedo HS, Malafaya PB, Sousa RA, Silva SS, *et al.* Natural origin biodegradable systems in tissue engineering and regenerative medicine: present status and some moving trends. J. R. Soc. Interface. 2007;4(17):999-1030.

56. Klein C, Driessen AA, Degroot K, Vandenhooff A. Biodegration behavior of various calcium phosphate materials in bone tissue. J Biomed Mater Res. 1983;17(5):769-84.

57. Temenoff JS, Mikos AG. Injectable biodegradable materials for orthopedic tissue engineering. Biomaterials. 2000;21(23):2405-12.

58. Burguera EF, Xu HHK, Weir MD. Injectable and rapid-setting calcium phosphate bone cement with dicalcium phosphate dihydrate. J Biomed Mater Res Part B. 2006;77B(1):126-34.

59. Xu HHK, Weir MD, Burguera EF, Fraser AM. Injectable and macroporous calcium phosphate cement scaffold. Biomaterials. 2006;27(24):4279-87.

60. Ginebra MP, Traykova T, Planell JA. Calcium phosphate cements as bone drug delivery systems: A review. J Control. Release. 2006;113(2):102-10.

61. Zhang S. Fabrication of novel biomaterials through molecular self-assembly. Nat Biotech. 2003;21(10):1171-8.

62. Scheller EL, Krebsbach PH, Kohn DH. Tissue engineering: state of the art in oral rehabilitation. J Oral Rehabil. 2009;36(5):368-89.

63. Segers VFM, Lee RT. Local delivery of proteins and the use of self-assembling peptides. Drug Discov Today. 2007;12(13-14):561-8.

64. Tsigkou O, Pomerantseva I, Spencer JA, Redondo PA, Hart AR, O'Doherty E, *et al*. Engineered vascularized bone grafts. Proc Natl Acad Sci U S A. 2010;107(8):3311-6.

65. Rahman CV, Saeed A. , White L. J., Gould T. W. A., Kirby G. T. S., Sawkins M. J., *et al.* Chemistry of polymer and ceramic-based injectable scaffolds and their applications in regenerative medicine. Chem Mater. 2012;24(5):781–95.

66. Park JB. The use of hydrogels in bone-tissue engineering. Medicina oral, patologia oral y cirugia bucal. 2011;16(1):e115-8.

67. Hou Q, De Bank P. A., M SK. Injectable scaffolds for tissue regeneration. J Mater Chem. 2004;14:1915-23.

68. Kretlow JD, Klouda L, Mikos AG. Injectable matrices and scaffolds for drug delivery in tissue engineering. Adv. Drug Delivery Rev. 2007;59(4-5):263-73.

69. Lee KY, Mooney DJ. Hydrogels for tissue engineering. Chem Rev. 2001;101(7):1869-79.

70. Lee KY, Rowley J, Eiselt P, Moy E. M, Bouhadir K. H., J. MD. Controlling mechanical and swelling properties of alginate hydrogels independently by cross-linker type and cross-linking density. Macromolecules. 2000;33(11):4291–4.

71. Hafeman AE, Li B, Yoshii T, Zienkiewicz K, Davidson JM, Guelcher SA. Injectable biodegradable polyurethane scaffolds with release of platelet-derived growth factor for tissue repair and regeneration. Pharm Res. 2008;25(10):2387-99.

72. Drury JL, Mooney DJ. Hydrogels for tissue engineering: scaffold design variables and applications. Biomaterials. 2003;24(24):4337-51.

73. Cui G, Li J, Lei W, Bi L, Tang P, Liang Y, *et al*. The mechanical and biological properties of an injectable calcium phosphate cement-fibrin glue composite for bone regeneration. J Biomed Mater Res Part B. Appl biomat. 2010;92(2):377-85.

74. Kai D, Prabhakaran MP, Stahl B, Eblenkamp M, Wintermantel E, Ramakrishna S. Mechanical properties and *in vitro* behavior of nanofiber-hydrogel composites for tissue engineering applications. Nanotechnology. 2012;23(9):095705.

75. Ye Q, Zund G, Benedikt P, Jockenhoevel S, Hoerstrup SP, Sakyama S, *et al*. Fibrin gel as a three dimensional matrix in cardiovascular tissue engineering. Eur J Cardiothorac Surg, 2000;17(5):587-91.

76. Shalaby WS, Park K. Biochemical and mechanical characterization of enzyme-digestible hydrogels. Pharm Res. 1990;7(8):816-23.

77. Hennink WE, van Nostrum CF. Novel crosslinking methods to design hydrogels. Adv. Drug Deliv. Rev. 2002;54(1):13-36.

78. Cai Q, Bei J, Wang S. Synthesis and degradation of a tri-component copolymer derived from glycolide, L-lactide, and epsilon-caprolactone. J Biomater Sci Polym Ed. 2000;11(3):273-88.

79. Lu L, Peter SJ, Lyman MD, Lai HL, Leite SM, Tamada JA, *et al*. *In vitro* degradation of porous poly(L-lactic acid) foams. Biomaterials. 2000;21(15):1595-605.

80. Lee KY, Alsberg E, Mooney DJ. Degradable and injectable poly(aldehyde guluronate) hydrogels for bone tissue engineering. J Biomed Mater Res. 2001;56(2):228-33.

81. Timmer MD, Ambrose CG, Mikos AG. *In vitro* degradation of polymeric networks of poly(propylene fumarate) and the crosslinking macromer poly(propylene fumarate)-diacrylate. Biomaterials. 2003;24(4):571-7.

82. Slaughter BV, Khurshid SS, Fisher OZ, Khademhosseini A, Peppas NA. Hydrogels in regenerative medicine. Adv Mat. 2009;21(32-33):3307-29.

83. Nguyen MK, Lee DS. Injectable biodegradable hydrogels. Macromol. Biosci. 2010;10(6):563-79.

84. Macaya D, Spector M. Injectable hydrogel materials for spinal cord regeneration: a review. Biomed. Mater. 2012;7(1):012001.

85. Nguyen MK, Lee DS. Injectable biodegradable hydrogels. Macromolecular bioscience. 2010;10(6):563-79.

86. Wong Po Foo CT, Lee JS, Mulyasasmita W, Parisi-Amon A, Heilshorn SC. Two-component protein-engineered physical hydrogels for cell encapsulation. Proc Natl Acad Sci U S A. 2009;106(52):22067-72. PMCID: 2791665.

87. Myung D, Waters D, Wiseman M, Duhamel PE, Noolandi J, Ta CN, *et al*. Progress in the development of interpenetrating polymer network hydrogels. Polym advan technol. 2008;19(6):647-57. PMCID: 2745247.

88. Park H, Kang SW, Kim BS, Mooney DJ, Lee KY. Shear-reversibly crosslinked alginate hydrogels for tissue engineering. Macromol Biosci. 2009;9(9):895-901.

89. Nuttelman CR, Mortisen DJ, Henry SM, Anseth KS. Attachment of fibronectin to poly(vinyl alcohol) hydrogels promotes NIH3T3 cell adhesion, proliferation, and migration. J Biomed Mater Res. 2001;57(2):217-23.

90. Sung HW, Huang DM, Chang WH, Huang RN, Hsu JC. Evaluation of gelatin hydrogel crosslinked with various crosslinking agents as bioadhesives: *in vitro* study. J Biomed Mater Res. 1999;46(4):520-30.

91. Crescenzi V, Francescangeli A, Taglienti A, Capitani D, Mannina L. Synthesis and partial characterization of hydrogels obtained via glutaraldehyde crosslinking of acetylated chitosan and of hyaluronan derivatives. Biomacromol. 2003;4(4):1045-54.

92. Tomihata K. IY. Crosslinking of hyaluronic acid with glutaraldehyde. J Polym Sci. 1997;35(16):3553-9.

93. Shen H, Hu X, Yang F, Bei J, Wang S. An injectable scaffold: rhBMP-2-loaded poly(lactide-co-glycolide)/hydroxyapatite composite microspheres. Acta Biomater. 2010;6(2):455-65.

94. Cohen S, Yoshioka T, Lucarelli M, Hwang LH, Langer R. Controlled delivery systems for proteins based on poly(lactic/glycolic acid) microspheres. Pharm Res. 1991;8(6):713-20.

95. Hu J, Sun X, Ma H, Xie C, Chen YE, Ma PX. Porous nanofibrous PLLA scaffolds for vascular tissue engineering. Biomaterials. 2010;31(31):7971-7. PMCID: 2930107.

96. Ma PX ZR. Synthetic nano-scale fibrous extracellular matrix. J Biomed Mater Res. 1999;46(1):60-72.

97. Mathiowitz E, Kline D, Langer R. Morphology of polyanhydride microsphere delivery systems. Scanning microscopy. 1990;4(2):329-40.

98. Rosca ID, Watari F, Uo M. Microparticle formation and its mechanism in single and double emulsion solvent evaporation. J Control. Release. 2004;99(2):271-80.

99. Vasir JK, Tambwekar K, Garg S. Bioadhesive microspheres as a controlled drug delivery system. Int J Pharm. 2003;255(1-2):13-32.

100. Mathiowitz E. BH, Giannos S., Dor P.,Turek T., Langer R. . Polyanhydride microspheres: IV. Morphology and characterization of systems made by spray drying. J Appl Polym Sci. 1992;45:125-34.

101. Felix Lanao RP, Leeuwenburgh SC, Wolke JG, Jansen JA. Bone response to fast-degrading, injectable calcium phosphate cements containing PLGA microparticles. Biomaterials. 2011;32(34):8839-47.

102. Pekarek KJ, Jacob JS, Mathiowitz E. Double-walled polymer microspheres for controlled drug release. Nature. 1994;367(6460):258-60.

103. Mainardes RM, Evangelista RC. PLGA nanoparticles containing praziquantel: effect of formulation variables on size distribution. Int J Pharm. 2005;290(1-2):137-44.

104. Berchane NS, Carson KH, Rice-Ficht AC, Andrews MJ. Effect of mean diameter and polydispersity of PLG microspheres on drug release: experiment and theory. Int J Pharm. 2007;337(1-2):118-26.

105. Bidarra SJ, Barrias CC, Fonseca KB, Barbosa MA, Soares RA, Granja PL. Injectable *in situ* crosslinkable RGD-modified alginate matrix for endothelial cells delivery. Biomaterials. 2011;32(31):7897-904.

106. Alsberg E, Anderson KW, Albeiruti A, Franceschi RT, Mooney DJ. Cell-interactive alginate hydrogels for bone tissue engineering. J Dent Res. 2001;80(11):2025-9.

107. Benoit DS, Anseth KS. The effect on osteoblast function of colocalized RGD and PHSRN epitopes on PEG surfaces. Biomaterials. 2005;26(25):5209-20.

108. Salinas CN, Anseth KS. The influence of the RGD peptide motif and its contextual presentation in PEG gels on human mesenchymal stem cell viability. J Tissue Eng Regen Med. 2008;2(5):296-304.

109. Hern DL, Hubbell JA. Incorporation of adhesion peptides into nonadhesive hydrogels useful for tissue resurfacing. J Biomed Mater Res. 1998;39(2):266-76.

110. Rizzi SC, Ehrbar M, Halstenberg S, Raeber GP, Schmoekel HG, Hagenmuller H, *et al*. Recombinant protein-co-PEG networks as cell-adhesive and proteolytically degradable hydrogel matrixes. Part II: biofunctional characteristics. Biomacromolecules. 2006;7(11):3019-29.

111. Sargeant TD, Desai AP, Banerjee S, Agawu A, Stopek JB. An *in situ* forming collagen-PEG hydrogel for tissue regeneration. Acta Biomater. 2012;8(1):124-32.

112. Seliktar D, Zisch AH, Lutolf MP, Wrana JL, Hubbell JA. MMP-2 sensitive, VEGF-bearing bioactive hydrogels for promotion of vascular healing. J Biomed Mater Res. A. 2004;68(4):704-16.

113. Lutolf MP, Weber FE, Schmoekel HG, Schense JC, Kohler T, Muller R, *et al*. Repair of bone defects using synthetic mimetics of collagenous extracellular matrices. Nat Biotechnol. 2003;21(5):513-8.

114. Rederstorff E, Weiss P, Sourice S, Pilet P, Xie F, Sinquin C, *et al*. An *in vitro* study of two GAG-like marine polysaccharides incorporated into injectable hydrogels for bone and cartilage tissue engineering. Acta Biomater. 2011;7(5):2119-30.

115. Liu X, Ma PX. The nanofibrous architecture of poly(L-lactic acid)-based functional copolymers. Biomaterials. 2010;31(2):259-69. PMCID: 2783301.

116. Liu X, Jin X, Ma PX. Nanofibrous hollow microspheres self-assembled from star-shaped polymers as injectable cell carriers for knee repair. Nat Mater. 2011;10(5):398-406. PMCID: 3080435.

117. Liu X, Smith LA, Hu J, Ma PX. Biomimetic nanofibrous gelatin/apatite composite scaffolds for bone tissue engineering. Biomaterials. 2009;30(12):2252-8.

118. Huang GTJ. Pulp and dentin tissue engineering and regeneration: current progress. Regen. Med. 2009;4(5):697-707.

119. Sun H-H, Jin T, Yu Q, Chen F-M. Biological approaches toward dental pulp regeneration by tissue engineering. J Tissue Eng Regen Med. 2011;5(4):e1-e16.

120. Huang GT. Dental pulp and dentin tissue engineering and regeneration: advancement and challenge. Front Biosci (Elite Ed). 2011;3:788-800.

121. Gronthos S, Brahim J, Li W, Fisher LW, Cherman N, Boyde A, *et al*. Stem cell properties of human dental pulp stem cells. J Dent Res. 2002;81(8):531-5.

122. Gronthos S, Mankani M, Brahim J, Robey PG, Shi S. Postnatal human dental pulp stem cells (DPSCs) *in vitro* and *in vivo*. Proc. Natl. Acad. Sci. 2000;97(25):13625-30.

123. Miura M, Gronthos S, Zhao M, Lu B, Fisher LW, Robey PG, *et al*. SHED: Stem cells from human exfoliated deciduous teeth. Proc. Natl. Acad. Sci. 2003;100(10):5807-12.

124. Seo B-M, Miura M, Gronthos S, Mark Bartold P, Batouli S, Brahim J, *et al*. Investigation of multipotent postnatal stem cells from human periodontal ligament. The Lancet. 2004;364(9429):149-55.

125. Shi S, Bartold PM, Miura M, Seo BM, Robey PG, Gronthos S. The efficacy of mesenchymal stem cells to regenerate and repair dental structures. Orthod Craniofac Res. 2005;8(3):191-9.

126. Huang GTJ, Sonoyama W, Liu Y, Liu H, Wang S, Shi S. The hidden treasure in apical papilla: the potential role in pulp/dentin regeneration and bioroot engineering. J Endod. 2008;34(6):645-51.

127. Sonoyama W, Liu Y, Fang D, Yamaza T, Seo B-M, Zhang C, *et al*. Mesenchymal stem cell-mediated functional tooth regeneration in swine. PLoS ONE. 2006;1(1):e79.

128. Sonoyama W, Liu Y, Yamaza T, Tuan RS, Wang S, Shi S, *et al*. Characterization of the apical papilla and its residing stem cells from human immature permanent teeth: a pilot study. J Endod. 2008;34(2):166-71.

129. Guo W, He Y, Zhang X, Lu W, Wang C, Yu H, *et al*. The use of dentin matrix scaffold and dental follicle cells for dentin regeneration. Biomaterials. 2009;30(35):6708-23.

130. Morsczeck C, Götz W, Schierholz J, Zeilhofer F, Kühn U, Möhl C, *et al*. Isolation of precursor cells (PCs) from human dental follicle of wisdom teeth. Matrix Biol. 2005;24(2):155-65.

131. Yamada Y, Nakamura S, Ito K, Kohgo T, Hibi H, Nagasaka T, *et al*. Injectable tissue-engineered bone using autogenous bone marrow-derived stromal cells for maxillary sinus augmentation: clinical application report from a 2-6-year follow-up. Tissue Eng Part A. 2008;14(10):1699-707.

132. Yoshimi R, Yamada Y, Ito K, Nakamura S, Abe A, Nagasaka T, *et al*. Self-assembling peptide nanofiber scaffolds, platelet-rich plasma, and mesenchymal stem cells for injectable bone regeneration with tissue engineering. J Craniofac Surg. 2009;20(5):1523-30.

133. Herberg S, Siedler M, Pippig S, Schuetz A, Dony C, Kim CK, *et al*. Development of an injectable composite as a carrier for growth factor-enhanced periodontal regeneration. J Clin Periodontol. 2008;35(11):976-84.

134. Kwon DH, Bennett W, Herberg S, Bastone P, Pippig S, Rodriguez NA, *et al*. Evaluation of an injectable rhGDF-5/PLGA construct for minimally invasive periodontal regenerative procedures: a histological study in the dog. J Clin Periodontol. 2010;37(4):390-7.

135. Ji QX, Chen XG, Zhao QS, Liu CS, Cheng XJ, Wang LC. Injectable thermosensitive hydrogel based on chitosan and quaternized chitosan and the biomedical properties. J Mater Sci. - Mater Med.2009;20(8):1603-10.

136. Ji QX, Deng J, Xing XAM, Yuan CQ, Yu XB, Xu QC, *et al*. Biocompatibility of a chitosan-based injectable thermosensitive hydrogel and its effects on dog periodontal tissue regeneration. Carbohydr Polym. 2010;82(4):1153-60.

137. Burdick JA, Anseth KS. Photoencapsulation of osteoblasts in injectable RGD-modified PEG hydrogels for bone tissue engineering. Biomaterials. 2002;23(22):4315-23.

138. Zhao L, Weir MD, Xu HHK. An injectable calcium phosphate-alginate hydrogel-umbilical cord mesenchymal stem cell paste for bone tissue engineering. Biomaterials. 2010;31(25):6502-10.

139. Chong SL, Mitchell R, Moursi AM, Winnard P, Losken HW, Bradley J, *et al*. Rescue of coronal suture fusion using transforming growth factor-beta 3 (Tgf-beta 3) in rabbits with delayed-onset craniosynostosis. Anat Rec Part A. 2003;274A(2):962-71.

140. Opperman LA, Moursi AM, Sayne JR, Wintergerst AM. Transforming growth factor-beta 3 (Tgf-beta 3) in a collagen gel delays fusion of the rat posterior interfrontal suture in vivo. Anat Rec 2002;267(2):120-30.

141. Moioli EK, Hong L, Guardado J, Clark PA, Mao JJ. Sustained release of TGF beta 3 from PLGA microspheres and its effect on early osteogenic differentiation of human mesenchymal stem cells. Tissue Eng. 2006;12(3):537-46.

142. Artzi N, Oliva N, Puron C, Shitreet S, Artzi S, bon Ramos A, *et al*. *In vivo* and *in vitro* tracking of erosion in biodegradable materials using non-invasive fluorescence imaging. Nat Mater. 2011;10(9):704-9. PMCID: 3160718.

143. Gao X, Chung LW, Nie S. Quantum dots for *in vivo* molecular and cellular imaging. Methods Mol Biol. 2007;374:135-45.

144. Larson DR, Zipfel WR, Williams RM, Clark SW, Bruchez MP, Wise FW, *et al*. Water-soluble quantum dots for multiphoton fluorescence imaging in vivo. Science. 2003;300(5624):1434-6.

145. Chen H-H, Anbarasan R, Kuo L-S, Chen P-H. Synthesis and characterizations of novel acid functionalized and fluorescent poly(ε-caprolactone). J Mater Sci. 2010;46(6):1796-805.

146. Sigma-Aldrich Co. LLC 2014 . Eosin Y. Retrieved from http://www.sigmaaldrich.com/catalog/product/sial/e4009?lang=en&region=US.

147. Prahl S. Biomedical Optics in Portland-Eosin Y, 2012.Reterieved from http://omlc.ogi.edu/spectra/PhotochemCAD/html/061.html.

148. Sigma-Aldrich Co. LLC 2014 . L-Lactide, Stannous octoate, Eosin Y. Retrieved respectively from http://www.sigmaaldrich.com/catalog/product/aldrich/303143?lang=en&region=US, http://www.sigmaaldrich.com/catalog/product/aldrich/s3252?lang=en&region=US http://www.sigmaaldrich.com/catalog/product/sial/e4009?lang=en&region=US.

149. Kaihara S, Matsumura S, Mikos AG, Fisher JP. Synthesis of poly(L-lactide) and polyglycolide by ring-opening polymerization. Nat Protocols. 2007;2(11):2767-71.

150. Dechy-Cabaret O, Martin-Vaca B, Bourissou D. Controlled ring-opening polymerization of lactide and glycolide. Chem Rev. 2004;104(12):6147-76.

151. Drumright RE, Gruber PR, Henton DE. Polylactic acid technology. Adv Mater. 2000;12(23):1841-6.

152. Chen JP, Cheng TH. Thermo-responsive chitosan-graft-poly(N-isopropylacrylamide) injectable hydrogel for cultivation of chondrocytes and meniscus cells. Macromol. Biosci.. 2006;6(12):1026-39.

153. Hans R K. Syntheses and application of polylactides. Chemosphere. 2001;43(1):49-54.

154. Platel RH, Hodgson LM, Williams CK. Biocompatible initiators for lactide polymerization. Polym Rev. 2008;48(1):11-63.

155. Kricheldorf HR, Kreiser-Saunders I, Stricker A. Polylactones 48. $SnOct_2$ initiated polymerizations of lactide: A mechanistic study. Macromolecules. 2000;33(3):702-9.

156. Nam YS, Park TG. Porous biodegradable polymeric scaffolds prepared by thermally induced phase separation. J Biomed Mater Res. 1999;47(1):8-17.

157. Ma PX, Zhang R. Synthetic nano-scale fibrous extracellular matrix. J Biomed Mater Res.1999;46(1):60-72.

158. Holzwarth JM, Ma PX. Biomimetic nanofibrous scaffolds for bone tissue engineering. Biomaterials. 2011;32(36):9622-9.

159. Smith LA, Ma PX. Nano-fibrous scaffolds for tissue engineering. Colloids Surf., B 2004;39(3):125-31.

160. Liu XH, Ma PX. Polymeric scaffolds for bone tissue engineering. Ann. Biomed. Eng.. 2004;32(3):477-86.

161. Vasita R, Katti DS. Nanofibers and their applications in tissue engineering. Int J Nanomedicine. 2006;1(1):15-30. PMCID: 2426767.

162. Smith LA, Liu X, Ma PX. Tissue engineering with nano-fibrous scaffolds. Soft Matter. 2008;4(11):2144.

163. Woo KM, Jun J-H, Chen VJ, Seo J, Baek J-H, Ryoo H-M, *et al*. Nano-fibrous scaffolding promotes osteoblast differentiation and biomineralization. Biomaterials. 2007;28(2):335-43.

164. Wang J, Liu X, Jin X, Ma H, Hu J, Ni L, *et al*. The odontogenic differentiation of human dental pulp stem cells on nanofibrous poly(l-lactic acid) scaffolds *in vitro* and *in vivo*. Acta Biomater. 2010;6(10):3856-63.

165. Wang J, Ma H, Jin X, Hu J, Liu X, Ni L, *et al*. The effect of scaffold architecture on odontogenic differentiation of human dental pulp stem cells. Biomaterials. 2011;32(31):7822-30.

166. Li Z, Wang C. Effects of working parameters on electrospinning. one-dimensional nanostructures: Springer; 2013. p. 15-28.

167. Woo KM, Jun JH, Chen VJ, Seo J, Baek JH, Ryoo HM, *et al*. Nano-fibrous scaffolding promotes osteoblast differentiation and biomineralization. Biomaterials. 2007;28(2):335-43.

168. Xu CY, Inai R, Kotaki M, Ramakrishna S. Aligned biodegradable nanofibrous structure: a potential scaffold for blood vessel engineering. Biomaterials. 2004;25(5):877-86.

169. Engelberg I, Kohn J. Physico-mechanical properties of degradable polymers used in medical applications: a comparative study. Biomaterials. 1991;12(3):292-304.

170. Gopferich A. Mechanisms of polymer degradation and erosion. Biomaterials. 1996;17(2):103-14.

171. Vert M, Mauduit J, Li S. Biodegradation of PLA/GA polymers: increasing complexity. Biomaterials. 1994;15(15):1209-13.